Redox Biology 66 (2023) 102848

Contents lists available at ScienceDirect

Redox Biology

journal homepage: www.elsevier.com/locate/redox

Protective effects of luteolin against amyloid beta-induced oxidative stress and mitochondrial impairments through peroxisome proliferator-activated receptor γ-dependent mechanism in Alzheimer's disease

Zhijun He [a,b], Xiaoqian Li [b], Zi Wang [b], Yingqi Cao [b], Shuangxue Han [b], Nan Li [b,c], Jie Cai [a,**], Shuiyuan Cheng [a], Qiong Liu [b,c,*]

[a] National R&D Center for Se-rich Agricultural Products Processing, Hubei Engineering Research Center for Deep Processing of Green Se-rich Agricultural Products, School of Modern Industry for Selenium Science and Engineering, Wuhan Polytechnic University, Wuhan, 430023, China
[b] Shenzhen Key Laboratory of Marine Biotechnology and Ecology, College of Life Sciences and Oceanography, Shenzhen University, Shenzhen, Guangdong, 518055, China
[c] Shenzhen-Hong Kong Institute of Brain Science-Shenzhen Fundamental Research Institutions, 518055, China

ARTICLE INFO

Keywords:
Luteolin
Alzheimer's disease (AD)
β-amyloid (Aβ)
Mitochondrial impairments
Apoptosis
Peroxisome proliferator-activated receptor γ (PPARγ)

ABSTRACT

Alzheimer's disease (AD) is a devastating neurodegenerative disorder characterized by the deposition of β-amyloid (Aβ) peptides and dysfunction of mitochondrion, which result in neuronal apoptosis and ultimately cognitive impairment. Inhibiting Aβ generation and repairing mitochondrial damage are prominent strategies in AD therapeutic treatment. Luteolin, a flavonoid compound, exhibits anti-inflammatory neuroprotective properties in AD mice. However, it is still unclear whether luteolin has any effect on Aβ pathology and mitochondrial dysfunction. In this study, the beneficial effect and underlying mechanism of luteolin were investigated in triple transgenic AD (3 × Tg-AD) mice and primary neurons. Our study showed that luteolin supplement significantly ameliorated memory and cognitive impairment of AD mice and exerted neuroprotection by inhibiting Aβ generation, repairing mitochondrial damage and reducing neuronal apoptosis. Further research revealed that luteolin could directly bind with peroxisome proliferator-activated receptor gama (PPARγ) to promote its expression and function. In the culture of hippocampus-derived primary neurons, addition of PPARγ antagonist GW9662 or knockdown of PPARγ with its siRNA could eliminate the effect of luteolin on AD pathologies. In summary, this work revealed for the first time that luteolin effectively improved cognitive deficits of 3 × Tg-AD mice and inhibited Aβ-induced oxidative stress, mitochondrial dysfunction and neuronal apoptosis via PPARγ-dependent mechanism. Hence, luteolin has the potential to serve as a therapeutic agent against AD.

1. Introduction

Alzheimer's disease (AD), one of most leading causes of death among the elderly over 65 years old, currently affects over 24 million of people worldwide, with roughly 5 million new cases every year [1–3]. The most manifest pathological feature of AD is the senile plaques formed by accumulation of amyloid β (Aβ) in the hippocampus, neocortex, and other brain regions essential for cognitive function [4]. Aβ peptides are derived from the sequential cleavage of amyloid protein precursor (APP), an important single-transmembrane protein, by γ-secretase and β-secretase (BACE1), which contributes markedly to the initiation and development of AD. Thus, BACE1 is considered as the rate-limiting enzyme for regulating the production of Aβ and inhibition of BACE1 transcription and activity could block the progression of AD [5–7].

Abbreviations: AD, Alzheimer's disease; Aβ, β-amyloid; APP, amyloid precursor protein; BACE1, β-Site APP-Cleaving Enzyme 1; Bcl-2, B-cell lymphoma-2; Bax, BCL2-related X protein; CytC, cytochrome *c*; Drp1, dynamin-related protein 1; DAPI, n-acetyl-diaminopimelate deacetylase; Fis1, Fission 1; IDE, insulin-degrading enzyme; Mfn2, mitofusin 2; MMP, mitochondrial membrane potential; NRF1, Nuclear respirator factor 1; NRF2, Nuclear respirator factor 2; PGC-1α, peroxisome proliferator-activated receptor gamma coactivator 1-alpha; PPARγ, peroxisome proliferator activated receptor gamma; ROS, reactive oxygen species; TFAM, mitochondrial transcription factor A; UCP2, uncoupling protein 2.

* Corresponding author. College of Life Sciences and Oceanography, Shenzhen University, Shenzhen, 518055, China.
** Corresponding author. School of Modern Industry for Selenium Science and Engineering, Wuhan Polytechnic University Wuhan, 430023, China.
E-mail addresses: caijievip@whpu.edu.cn (J. Cai), liuqiong@szu.edu.cn (Q. Liu).

https://doi.org/10.1016/j.redox.2023.102848
Received 21 July 2023; Received in revised form 10 August 2023; Accepted 11 August 2023
Available online 12 August 2023

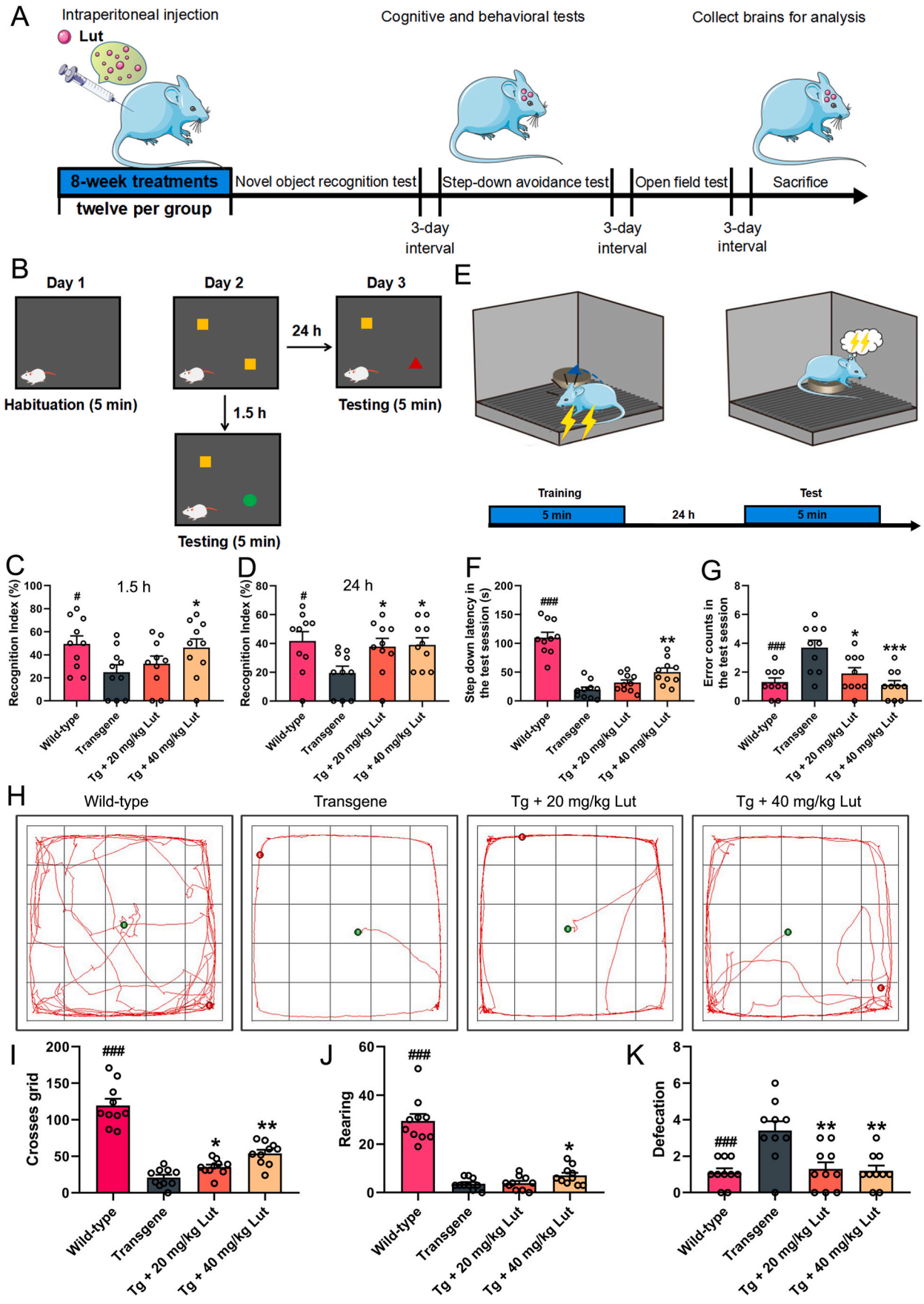

(caption on next page)

Fig. 1. Attenuation of cognitive impairments by luteolin in 3×Tg-AD mice. (**A**) Study design of animal experiments. 10-month-old 3 × Tg-AD mice (Transgene, Tg) were intraperitoneally administrated luteolin for 8 weeks and then the exploratory behavior and cognitive ability were evaluated by novel object recognition task, step-down avoidance test and open field test in turn. (**B**) Illustration of novel object recognition task. (**C-D**) Assessing the effects of luteolin on recognition index (%) in testing stage after 1.5 h and 24 h. (**E**) Schematic diagram of step-down avoidance test. (**F-G**) Step down latency and error counts during the test session. **(H)** The representative moving paths for the mice in the open field test during the 5 min test period. **(I–K)** The number of crossed grids, frequencies of rearing and amount of defecation in the open field test. #: WT group vs. Tg group; *: Tg + Lut group vs. Tg group. n=10 mice; $^{\#}P < 0.05$ and $^{\#\#\#}P < 0.001$, $^{*}P < 0.05$, $^{**}P < 0.01$ and $^{***}P < 0.01$, respectively.

Insulin-degrading enzyme (IDE) is an important enzyme that regulates the degrees of insulin and Aβ peptides, which, in addition to Aβ degradation, is critical for Aβ homeostasis [8]. Recent research has shown that dysregulation of IDE results in a >50% decline of Aβ clearance in both brain of AD mice and primary hippocampal neurons [9,10]. Therefore, targeting IDE has been regarded as an attractive therapeutic strategy against AD in terms of accelerating Aβ clearance [10].

The deposition of Aβ can causes a series of downstream cascades containing oxidative stress, endoplasmic reticulum stress, mitochondrial dysfunction and neuronal apoptosis, which eventually leads to cognitive impairment [10,11]. Mitochondria, a core organelle, is responsible for multiple biological functions including energy metabolism, biosynthesis, calcium buffering, stress responses, signaling modulation, neuronal and synaptic function [12,13]. Mitochondrial abnormalities containing aberrant mitochondrial membrane potential (MMP), impaired mitochondrial dynamics, abnormal mitochondrial gene expression, defective biogenesis, vulnerability to oxygen-glucose deprivation, and reactive oxygen species (ROS) overproduction are directly linked to AD-related pathology [14–16]. Studies have demonstrated that Aβ could directly or indirectly impair the morphology and function of mitochondria, leading to the induction of mitochondrial oxidative stress and the activation of intrinsic apoptotic signaling pathway cascade both in AD-related cell lines and AD mice [17–19]. For instance, Aβ could increase mitochondrial oxidative stress and activate mitochondrial apoptotic pathway in HL-1 cells and $A\beta_{1\text{-}42}$-injected mice. In addition, these processes in themselves help to accelerate Aβ generation, further exacerbating mitochondrial dysfunction and leading to a vicious cycle, eventually resulting in neuronal degeneration and apoptosis [20]. Thus, suppression of mitochondrial impairment is considered critical for improving the pathological damage in AD.

Peroxisome proliferator-activated receptor gamma (PPARγ), a pivotal nuclear receptor, regulates the transcription of all sorts of genes involved in cell differentiation, inflammation, oxidative stress, lipid metabolism and glucose homeostasis [10,21,22]. A growing body of evidence demonstrates that BACE1 expression can be inhibited via binding PPARγ response element to the promoter region of the BACE1 gene, subsequently suppressing Aβ generation [23,24]. Interestingly, we have recently reported that esculentoside A can reduce the production of Aβ by activating PPARγ to prevent the expression of BACE1 in AD mice as well as neurons [10]. Many researches have provided ample proof that PPARγ could regulate mitochondrial function in multiple models of central nervous system diseases [25–28]. For example, ligustrazine piperazine derivative, a novel PPARγ agonist, is able to enhance brain glucose metabolism and improve cognitive deficits by regulating mitophagy in a PPARγ-dependent manner in APP/PS1 mice. Therefore, PPARγ is a promising target and PPARγ agonists may serve as good candidates for the treatment of AD.

A series of researches have fastened on natural compounds to confirm potential drug candidates for AD treatment [29]. Luteolin (3′,4′,5,7-tetrahydroxy flavones), a natural flavonoid widely found in many medical herbs, has shown conspicuous anti-inflammatory, anti-oxidant, anti-apoptotic and neuroprotective activities [30–32]. According to recent studies, luteolin exerts its biological functions by regulating PPARγ activity both in vivo and in vitro [33,34]. For instance, luteolin improves inflammation and autophagy induced by cerebral ischemia/reperfusion via activating PPARγ in the hippocampus of rats. More recently, it was found that luteolin significantly inhibited ER stress and neuroinflammation in AD mice [30]. However, whether luteolin affects the mitochondrial impairments in AD remains to be further elucidated.

To develop an effective clinical drug, an adequate understanding of the mechanism of action of luteolin must be entrenched in preclinical models of AD. In the present study, the effects and mechanism of luteolin on Aβ pathology, oxidative stress and mitochondrial function were investigated in 3 × Tg-AD mice in vivo, as well as the primary neurons in vitro. It was found that luteolin effectively improved cognitive impairment by restraining Aβ production, promoting Aβ degradation, reducing oxidative stress and inhibiting mitochondrial damage-caused neuronal apoptosis through a PPARγ-dependent mechanism.

2. Materials and methods

2.1. Chemicals and reagents

Luteolin (purity ≥98%) and $A\beta_{1\text{-}42}$ peptide were acquired from Sigma-Aldrich (St. Louis, MO, USA). Foetal Bovine Serum (FBS), DMEM high-glucose medium, B27 and antibiotics (penicillin and streptomycin) were obtained from Gibco (Grand Island, NY, USA). Superoxide dismutase (SOD) assay kit and malondialdehyde (MDA) assay kit were purchased from Nanjing Jiancheng Bioengineering Institute (Nanjing, China). Glutathione (GSH) test kit, Pierce BCA protein assay kit and reactive oxygen species (ROS) test kit were provided by Beyotime Biotechnology (Shanghai, China). GW9662 (PPARγ inhibitor) was purchased from MedChemExpress (Monmouth Junction, NJ, USA).

2.2. Experimental mice and pharmacological treatment

3 × Tg-AD mice carrying the human mutations of APPswe, $PS1_{M126V}$ and Tau_{P301L} (strain: B6; 129-$Psen1^{tm1Mpm}$ Tg [APPSwe, tauP301L] 1Lfa/Mmjax) were acquired from Jackson Laboratory (Bar Harbor, ME, USA). Wild-type (WT) mice (strain: B6129SF2/J) were used as controls. Mice were maintained in ventilated cages with a temperature of 22–23 °C and relative humidity of 55%–60% with a 12-h light/12-h dark cycle. The water and standard food pellets were available *ad libitum*. All animal care and experiments were carried out strictly according to the guidance of the Institutional Animal Care and Use Committee of the Institute of Nutritional Sciences in China upon approval by the Regional Ethical Committee for Animal Experimentation at Shenzhen University (Permit Number: AEWC-20140615-002).

Female 8-month-old 3 × Tg-AD mice and age-matched WT mice were randomly divided into the following four groups (12 mice per group): untreated WT mice (Wild-type group), untreated AD mice (Transgene group), AD mice receiving treatment with a low dosage of 20 mg/kg luteolin (Tg + 20 mg/kg Lut group), and AD mice receiving treatment with a high dose of 40 mg/kg luteolin (Tg + 40 mg/kg Lut group). Mice in the treated AD group were given intraperitoneal injections of luteolin for 8 consecutive weeks. After the last luteolin treatment, behavioral tests were carried out for 12 days and then the mice were sacrificed. The experimental procedures for the in vivo study were illustrated in Fig. 1A.

2.3. Behavioral tests

After luteolin treatment, the behavioral manifestation of 3 × Tg-AD and WT mice were assessed with the novel object recognition (NOR) task, step-down avoidance test, and open field test in turn. The interval between the two tests was 3 days (Fig. 1A).

The NOR task, step-down avoidance test and open field test were

conducted as described previously [35,36]. For the NOR task, the time it took the mice spent on object A (yellow) refers to familiar (F), while that on new object B (red) or C (green) means new (N). The memory ability of the mice was reflected by recognition index (RI), which was calculated with the following formula: RI=N/(N+F). For step-down avoidance test, mice received electrical shock and quickly performed an instinctive reaction to jump onto the insulative platform to avoid the electric stimulation. The time it took the mice to step down from the insulated platform onto the grid (step-down latency) and number of times that the mice stepped down from platform (error counts) within 5 min were recorded. For open field test, the mice was located in the center of the floor in the apparatus and allowed to free explore the apparatus for consecutive 5 min after a 1-min acclimatization period. Numbers of grid crossings, rearing events, and defecation within 5 min in the open apparatus were recorded. The movements of the mice throughout the trials were automatically monitored using a camera connected to a computerized tracking system (Smart V3.0, RWD, Shenzhen, China) and further analyzed with the ANY-MAZE software.

2.4. Tissue preparation and protein extraction

The animals were deeply anesthetized with isoflurane and euthanized. Brains were rapidly harvested, washed with normal saline and then separated into left and right hemispheres sagittally. Left hemispheres were immersion-fixed in 4% paraformaldehyde (PFA) overnight at 4 °C, transferred to 30% sucrose solution, and then embedded in paraffin. The hemispheres were cut into 5 μm sliced sections and used for histological analysis. The hippocampi from right hemispheres in each group were homogenized in radio immunoprecipitation assay (RIPA) lysis solution containing 1 mM phenylmethylsulfonyl fluoride (PMSF; Thermo Scientific, USA) supplemented with phosphatase and proteinase inhibitors. Subsequently, the homogenates were centrifuged at 12,000 rpm for 20 min at 4 °C. The supernatants were collected and used for further experiments.

2.5. Transmission electron microscopy (TEM) analysis

TEM was conducted as previously described [36]. Briefly, mouse hippocampal tissues were fixed with 2.5% glutaraldehyde and 1% osmium tetroxide for 2 h at 4 °C, and then dehydrated in graded ethanol solutions (50%, 70% and 90%). The tissues were embedded in epoxy resin, sectioned into 70 nm ultrathin sections using an ultramicrotome (Leica EM UC6), and stained with 2% uranyl acetate for 5 min and 2% lead citrate for 15 min. TEM images were photographed using a transmission electron microscope (FEI Tecnai G2 Spirit).

2.6. Primary neuron culture

Primary neurons were obtained from the hippocampus of newborn WT or AD mice (postnatal day 0–2) and cultured at a certain concentration for diverse cell experiments. Hippocampi tissue was dissected into 1 mm^3 pieces and then digested with papain for 30 min at 37 °C. Next, the tissue was blown gently for 8–10 times in culture medium (supplemented with 98% DMEM, 1% penicillin/streptomycin and 1% rat serum) and the dissociated neurons were seeded in cell culture plates precoated with poly-D-lysine (Sigma, USA). After 3–6 h, the culture medium was replaced with new neurobasal medium containing 0.2% glutamate, 1% penicillin/streptomycin and 2% B27 for further culture. The primary neurons were maintained in the incubator (5% CO_2 and 95% humidity) at 37 °C for 9 consecutive days and half of the old culture medium was replaced with new neurobasal medium every three days. At day 10, the primary neurons were treated with luteolin (2.5 and 5 μM, respectively) or Aβ (10 μM) for 24 h. The concentration of GW9662 used for treating primary neurons was 20 μM in this study.

2.7. Preparation of Aβ oligomer

Human $A\beta_{1–42}$ peptide was dissolved in 1,1,1,3,3,3-hexafluoroisopropanol (HFIP) and sonicated for 30 min to get a limpid solution. Then, HFIP was removed through lyophilization and the obtained $A\beta_{1-42}$ monomer powder was dissolved in sterile dimethyl sulfoxide (DMSO) at 2 mM. For $A\beta_{1-42}$ oligomer (AβO) preparation, a concentration of 2 mM $A\beta_{1–42}$ was diluted with cultured medium and then incubated overnight at 4 °C before usage.

2.8. Cell viability assay

Cell viability was measured by the Cell Counting Kit-8 (CCK-8) assay. In short, primary neurons were seeded in 96-well plates and cultured for 9 days, and then treated with luteolin at various concentrations for another 24 h. After incubation, primary neurons were incubated with CCK-8 for 24 h at 37 °C. The absorbance was detected at 450 nm using a spectra microplate reader (Thermo Fisher Scientific, Hudson, NH, USA).

2.9. Determination of mitochondrial membrane potential (MMP)

The MMP in primary neurons was measured using a 5, 5′, 6, 6′-tetrachloro-1,1′3,3′-tetrathylbenzimidazolyl-carbo-cyanine iodide (JC-1) MMP detection kit (Beyotime, Shanghai, China). Primary neurons were cultured in confocal dishes for 9 days and then treated with $A\beta_{1–42}$ and luteolin for another 24 h. Subsequently, the old neurobasal mediums were removed and primary neurons were incubated with JC-1 staining working solution for 20 min, followed by washing three times with JC-1 staining buffer. Finally, new neurobasal medium was added to the confocal dishes and fluorescence intensity was detected using a confocal laser scanning microscope (Zeiss, Jena, Germany). The relative fluorescence ratio of red and green was applied to evalute the level of mitochondrial depolarization.

2.10. Cell apoptosis assay

Terminal deoxynucleotidyl transferase-mediated deoxyuridine triphosphate nick-end labeling (TUNEL) staining was performed to measure neuronal apoptosis using the In Situ Cell Death Detection Kit (Roche, Mannheim, Germany) following the manufacturer's protocols. Briefly, primary neurons were pretreated with 20 μg/mL protease K for 20 min at 37 °C, following washed three times with PBS. Thereafter, primary neurons were incubated with TUNEL reaction mixture in the dark for 1 h at 37 °C and then stained with 4′,6-diamidino-2-phenylindole (DAPI) for 8 min. After washing in PBS three times, primary neurons were imaged using a confocal laser scanning microscope (LSM880; Zeiss, Jena, Germany). The fluorescence intensity of TUNEL staining were quantified with the Image-Pro Plus software (Version 6.0; Media Cybernetics, Bethesda, USA).

2.11. Immunofluorescent staining

For immunofluorescence staining of sections, brain paraffin sections in different groups were permeabilized with 1% Triton X-100 in (Beyotime, Shanghai, China) PBS at room temperature for 20 min and blocked with blocking solution (1% Triton X-100 and 10% goat serum in PBS) at 37 °C for 2 h. Subsequently, the sections were incubated with primary antibodies (summarized in Supplementary Table 1) at 4 °C overnight. After rinsing thrice with PBS, sections were incubated with fluorescence-labeled secondary antibody (anti-rabbit Alexa 488, and anti-mouse Alexa 555, 1:1000 diluted in blocking buffer; Abcam, Cambridgeshire, England) for 2 h at room temperature in darkness, followed by washing thrice with PBS. Finally, the nucleus were counterstained with DAPI (1:1000; Beyotime, Shanghai, China) for 20 min, and coverslips were mounted onto microscope slides. For immunofluorescence staining of primary neurons, cultured neurons were fixed with 4% PFA

for 30 min, permeabilized with 0.2% Triton X-100 in PBS at room temperature for 10 min, and then blocked with blocking solution for 2 h. Subsequently, neurons were incubated with primary antibody (summarized in Supplementary Table 1) for overnight at 4 °C, followed by incubating with secondary antibodies for 2 h. After washing in PBS, the neurons were counterstained with DAPI for 8 min, and then rinsed thrice with PBS. Fluorescence images of brain sections and neurons were acquired under a confocal laser scanning microscope (LSM880; Zeiss, Jena, Germany). The optics of the microscope was adjusted to avoid any potential crosstalk of signals between different channels. All image analyses were performed using the Image-Pro Plus software (Version 6.0; Media Cybernetics, Bethesda, USA). For quantification of the intensity, images obtained under the same staining and imaging conditions were used. These pictures were converted to grayscale 8-bit images and we quantified the fluorescence intensity of these proteins by setting the threshold of the intensity to 100–255 and binarizing them. Finally, the data were normalized with the value of the samples in AD group and the graphs were generated by the GraphPad Prism 8.0 software.

2.12. Knockdown of PPARγ by small interfering RNA

The primary hippocampal neurons were transfected with small interfering RNA (siRNA)-PPARγ or siRNA-scrambled (General Biosystems, Anhui, China) by Lipofectamine 2000 reagent (Invitrogen, Carlsbad, California, USA). The sequences used of PPARγ siRNA was as follows: 5′-UCCACACUAUGAAGACAUUTT-3′ and 5′-AAUGUCUUCAUAGUGUGGATT-3′ (antisense). Twenty-four hours after transfection, knockdown of PPARγ expression was analyzed with qPCR and Western blotting. GAPDH was included as an internal control.

2.13. RNA extraction and quantitative real-time PCR performance

Total RNA was extracted from the hippocampus of mice and primary neurons using the RNeasy MiniKit (Qiagen), following to the manufacturer's instructions. RNA concentrations were equalized and reverse-transcribed into cDNA using a High-Capacity cDNA Archive kit (Vazyme, Nanjing, China). Quantitative real-time PCR assays were conducted with a 7500 Real-time PCR System (Applied Biosystems) using total RNA and the ChamQTM SYBR Color qPCR Master Mix (Vazyme, Nanjing, China). Primers were designed using NCBI/Primer-BLAST software and listed in Supplementary Table 2. Quantification of qPCR signals was performed using ΔΔCt relative quantification method with GAPDH as a reference gene.

2.14. Western blot analysis

Protein concentrations were detected using a pierce BCA protein assay kit. 25 μg extracted protein in each hole were separated by 10–15% SDS-polyacrylamide gel electrophoresis and then transferred onto 0.45 μm polyvinylidene difluoride membranes (PVDF; Millipore, USA). Subsequently, the membranes were blocked with 5% skim dry milk for 2 h, following by incubating at 4 °C overnight with corresponding primary antibodies (summarized in Supplementary Table 1). After washing thrice with Tris-buffered saline with Tween 20 (TBST), the membranes were incubated with secondary antibodies (goat anti-mouse and goat anti-rabbit) in TBST for 2 h at at room temperature. After incubation, the blots were developed by an enhanced chemiluminescence (ECL) kit (Thermo Scientific, USA) and then scaned using a Tanon 5200 imaging system (Tanon, China). The intensity of immunoreactive band was analyzed using ImageJ software.

2.15. Determination of ROS levels

The levels of ROS in hippocampal neurons following Aβ stimulation were assessed with a fluorescent probe 2′,7′-dichlorfluorescein-diacetate (DCFH-DA) kit (Beyotime, Shanghai, China). Briefly, the old cultured medium was removed from hippocampal neurons and every well was washed with PBS. Then, the neurons were cultured in serum-free medium containing 10 μM DCFH-DA dye in the dark for 20 min at 37 °C. After incubation, hippocampal neurons were washed twice times with PBS to eliminate the extracellular DCFH-DA. The mean fluorescence intensity was detected at 488-nm excitation and 535-nm emission wavelengths by an Accuri C6 flow cytometry (Beckman Coulter, Brea, CA, USA).

2.16. Determination of SOD activity, MDA and GSH levels

Brain tissues and primary neuron were homogenized and centrifuged at 12,000 rpm for 20 min at 4 °C. Then, the supernatant was collected and the concentration of total protein was determined with a BCA assay kit. The activity of SOD and the levels of MDA and GSH were evaluated with SOD, MDA and GSH assay kits according to the manufacturer's protocols, respectively.

2.17. Molecular docking

Molecular docking of luteolin with PPARγ ligand binding domain was performed using the software of AutoDock 4.2.6. Three-dimensional structure of PPARγ was acquired from Protein Data Bank (http://www.rcsb.org/pdb; PDB ID: 2Q5S) and the structure of luteolin was obtained from PubChem database. Before molecular docking, protein (PPARγ) and Ligand (luteolin) files were converted to PDBQT format by ADFR 1.0 program. A grid box of $60 \times 60 \times 60$ Å^3 also was established and it could cover entire binding pocket. During molecular docking, the luteolin ligand and the PPARγ protein were set to be flexible and rigid, respectively. Lamarckian genetic algorithm was used to acquire the best binding pose of luteolin. Ultimately, the pose with lowest score was obtained from the docking results for further visualized analysis by softwares of PyMol-open-source and Maestro of academic edition.

2.18. Bio-layer interferometry to investigate molecular interaction

The interactions between luteolin and PPARγ were determined using the ForteBio Octet RED384 system (ForteBio Inc., CA, USA). Experiments were performed at room temperature according to the ForteBio manufacturer's recommendations. First, PPARγ protein was labeled with biotin for 30 min at room temperature, and then PD-10 desalting column (Thermo Scientific, USA) was used to eliminate the unconjugated biotin. Next, the sensors were prewetted in dialysis buffer and immersed in the biotinylated PPARγ solution for 15 min. The unloaded biotinylated PPARγ was selected as controls to calibrate the baseline drift. Finally, PPARγ were reacted with luteolin solution, which was prepared in a series of dilutions (3.125, 6.25, 12.5, 25, and 50 μmol/L) at room temperature. The data were analyzed by the analysis software accompanying the Octet Red384 Data analysis system (version 11.0, ForteBio).

2.19. Statistical analysis

Results are presented as means ± standard error of the mean (SEM). All statistical analyses were conducted using GraphPad Prism 8.0 software. Differences between groups were analyzed utilizing one way analysis of variance (ANOVA), followed by the bonferroni post hoc test. A $p < 0.05$ was required for results to be considered statistically significant.

3. Results

3.1. Luteolin improved cognitive ability in 3 × Tg-AD mice

The behavioural performances of experimental mice in four groups were assessed using three different behavioral tests. Novel object

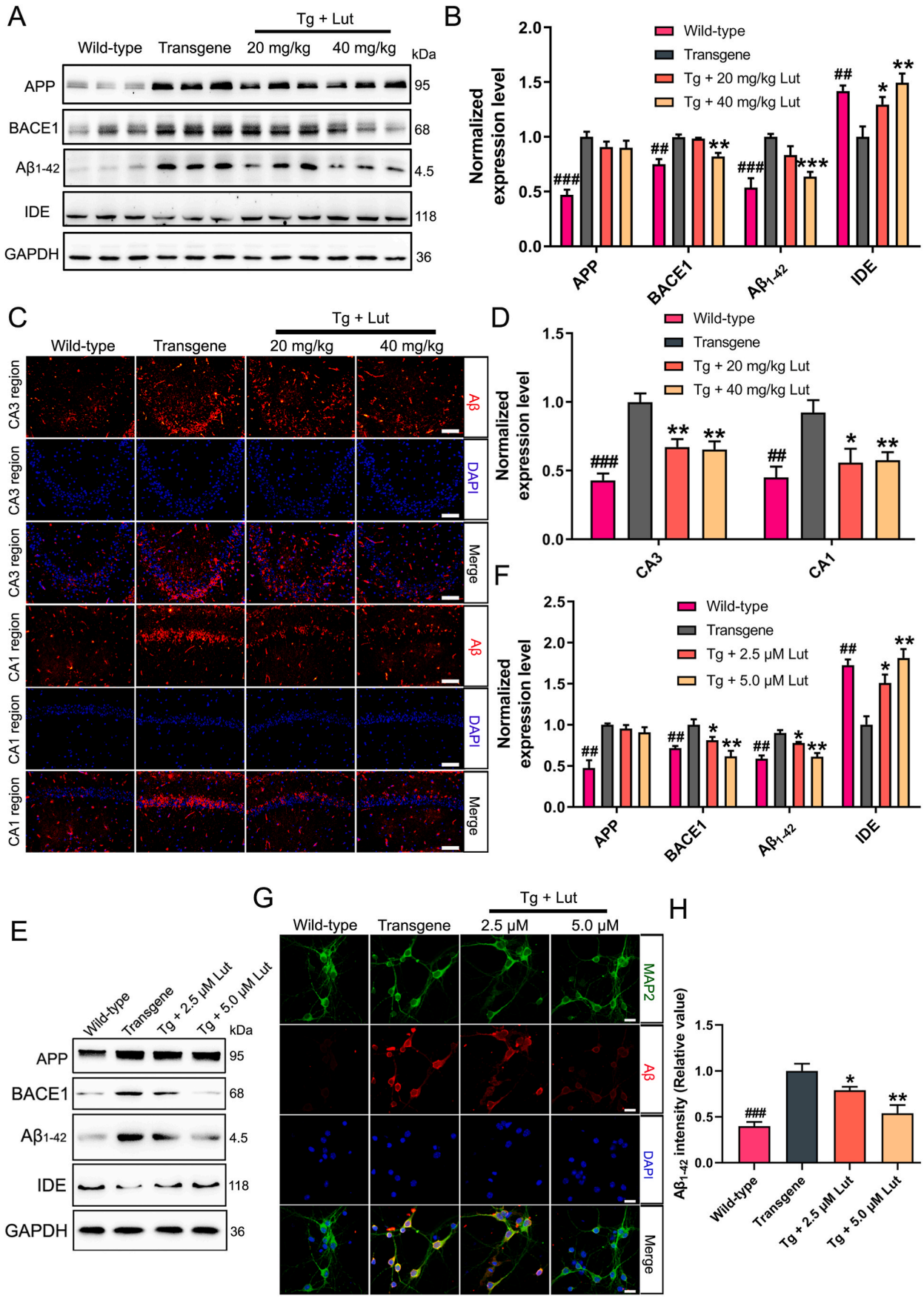

(caption on next page)

Fig. 2. Decrease of Aβ generation and accumulation by luteolin in 3×Tg-AD mice and primarily cultured neurons. (A) Representative results of Western blot analysis displayed the degrees of APP, BACE1, $A\beta_{1-42}$ and IDE in hippocampus of mice in WT, Tg and Tg + Lut group. **(B)** Quantification of these proteins were normalized to the degrees of GAPDH. **(C–D)** Representative immunofluorescent images showed the levels of Aβ in CA3 and CA1 regions of the hippocampus (Scale bar: 100 μm). Quantitative analysis of fluorescence intensity of Aβ in these regions. **(E–F)** Representative results of Western blot analysis showed the levels of APP, BACE1, $A\beta_{1-42}$ and IDE in primary hippocampal neurons. Quantification results were normalized against the levels of GAPDH. **(G–H)** Representative immunofluorescent images displayed the expression levels of Aβ in primary hippocampal neurons (Scale bar: 20 μm). The staining intensity of Aβ was quantified. #: WT group vs. Tg group; *: Tg + Lut group vs. Tg group. n=6 mice/wells per group; $^{\#\#}P < 0.01$, $^{\#\#\#}P < 0.001$, $^{*}P < 0.05$, $^{**}P < 0.01$ and $^{***}P < 0.001$, respectively.

recognition task and step-down avoidance test were used to evaluate the effect of luteolin on learning and memory of the 10-month-old 3 × Tg-AD mice. In novel object recognition test, AD mice exhibited a poor performance as evidenced by spending significantly less time exploring the new objects (B and C) compared with that exhibited by WT mice. However, luteolin obviously increased the time of AD mice spending on exploring the new objects. The RI value, an important indicator for reflecting the memory ability of mice, was calculated and the results showed that 40 mg/kg luteolin remarkably elevated RI levels during the 1.5 h retention test and both 20 and 40 mg/kg greatly elevated RI during the 24 h retention test (Fig. 1B–D). In step-down avoidance test, AD mice exhibited shorter step down latency and more error counts than those of WT mice, while luteolin treatment remarkably elevated the latency and reduced the error counts in a dose-dependent manner, showing improved cognitive impairment in this test (Fig. 1E–G).

The open-field test was used to assess the effect of luteolin on locomotor, exploration and anxiety degree of AD mice. In the open-field test, AD mice exhibited stronger degree of anxiety and weaker exploration ability, as evidenced by increased times of defecation and decreased numbers of crossed grids and rearing by comparing with WT mice. Luteolin dramatically improved the exploration and anxiety behaviors of AD mice in a dose-dependent manner, as indicated by remarkably reduced defecation frequencies, increased grid crossings and rearing frequencies (Fig. 1H–K). Thus, these results demonstrated that luteolin rescued cognitive deficits and meliorated the degree of anxiety, locomotor and exploration ability in 3 × Tg-AD mice.

3.2. Luteolin reduced Aβ generation and accumulation in 3 × Tg-AD mice and primary neurons

To investigate the effects of luteolin on Aβ pathology, the levels of APP, BACE1, $A\beta_{1-42}$ and IDE in hippocampus were measured using Western blot analysis. The levels of APP, BACE1 and $A\beta_{1-42}$ were dramatically increased and the level of IDE was greatly decreased in 3 × Tg-AD mice when compared with those in WT mice. Treatment with luteolin in the AD mice remarkably suppressed the levels of BACE1 and $A\beta_{1-42}$, but grew the level of IDE (Fig. 2A and B). Immunofluorescence staining with anti-Aβ antibody was performed to assess the impact of luteolin on Aβ deposition in hippocampus. As shown in Fig. 2C and D, the Aβ immunoreactivity in the CA1 and CA3 regions of hippocampi of 3 × Tg-AD mice were markedly larger than that in WT mice, and were significantly reduced after luteolin administration.

To further evaluate the role of luteolin on Aβ generation and clearance in vitro, the primary hippocampal neurons of 3 × Tg-AD mice were treated with luteolin at concentrations of 2.5 and 5 μmol/L, and the expression levels of APP, BACE1, $A\beta_{1-42}$ and IDE were analyzed by Western blot. As illustrated in Fig. 2E and F, luteolin remarkably reduced the levels of BACE1, and $A\beta_{1-42}$, while increased the level of IDE. Consistent with the results of Western-blot, immunofluorescence of Aβ and MAP2 (a neuronal marker) double labeling also showed that luteolin reduced the intensity of Aβ in primary neurons (Fig. 2G and H). The concentrations of luteolin in primary neurons treatment were selected according to the result of cell viability measurement (Supplementary Fig. 1). Based on these results, it could be concluded that luteolin reduced Aβ deposition by downgrading the expression level of BACE1 and upregulating the level of IDE.

3.3. Luteolin inhibited oxidative stress in 3 × Tg-AD mice and primary neurons

Many studies have indicated that oxidative stress caused by Aβ plays a critical role in pathological process of AD. To determine whether luteolin exerted antioxidant effects, the activity of SOD and the levels of MDA and GSH were measured in the hippocampi of 3 × Tg-AD mice. As shown in Fig. 3A–C, the concentrations of MDA were significantly grown, while the activity of SOD and the levels of GSH were greatly declined in the hippocampi of AD mice when compared with those in WT mice. Luteolin treatment remarkably grew both SOD activity and GSH level, but stopped the level of MDA. UCP2, a key mediator of oxidative damage, is part of a mechanism preventing ROS production, and plays a vital role in protecting neurons from oxidative stress [37]. The protein levels of UCP2 in the hippocampi of AD mice were detected using Western blot analysis. According to Fig. 3D and E, the expression levels of UCP2 were greatly decreased in AD mice compared to WT mice, while luteolin treatment obviously increased the levels of UCP2. In agreement with this, the immunofluorescence staining also showed that the level of UCP2 in the CA3 region of hippocmapus of AD mice were much lower than that in WT mice, whereas luteolin treatment greatly increased the fluorescence intensity of UCP2 (Fig. 3F and G).

In order to further investigate the anti-oxidant effects of luteolin in vitro, the levels of ROS and UCP2 were measured. As expected, the level of ROS was distinctly increased and the level of UCP2 was remarkably decreased in Aβ-induced primary neurons by comparing to control neurons. However, after the treatment with different doses of luteolin, the production of intracellular ROS was greatly suppressed and the expression level of UCP2 was significantly enhanced (Fig. 3H–J). Meanwhile, consistent with this results in vivo, luteolin also markedly reduced the level of MDA and enhanced the level of GSH and the activity of SOD in Aβ-stimulated primary neurons (Supplementary Fig. 2). To sum up, our results indicated that luteolin could ameliorate Aβ-induced oxidative stress both in vivo and vitro.

3.4. Luteolin enhanced mitochondrial biogenesis in 3 × Tg-AD mice and primary neurons

Suppression of mitochondrial biogenesis results in a series of impairments of mitochondrial function in AD. In order to see whether luteolin could affect the mitochondrial biogenesis, the expression levels of mitochondrial biogenesis-related proteins including peroxisome proliferator-activated receptor gamma coactivator 1-alpha (PGC-1α), nuclear respirator factor 1 (NRF1), nuclear respirator factor 2 (NRF2) and mitochondrial transcription factor A (TFAM) were measured both in AD mice and Aβ-induced primary neurons via Western blot analysis. As expected, the levels of PGC-1α, NRF1, NRF2 and TFAM were greatly decreased in the hippocampus of AD mice compared with WT mice, and luteolin administration significantly increased the degrees of these four proteins (Fig. 4A and B). Similarly, luteolin also increased the levels of PGC-1α, NRF1, NRF2 and TFAM in Aβ-induced primary hippocampal neurons (Fig. 4E and F). To verify these Western blotting results, immunofluorescent assay were performed to show the levels of NRF2 in the CA1 region of the hippocampus. As shown in Fig. 4C and D, the degrees of NRF2 was greatly declined in AD mice by comparing to WT mice, while luteolin treatment obviously increased the intensity of NRF2 in the CA1 region. Collectively, these results suggested that luteolin enhanced the process of mitochondrial biogenesis.

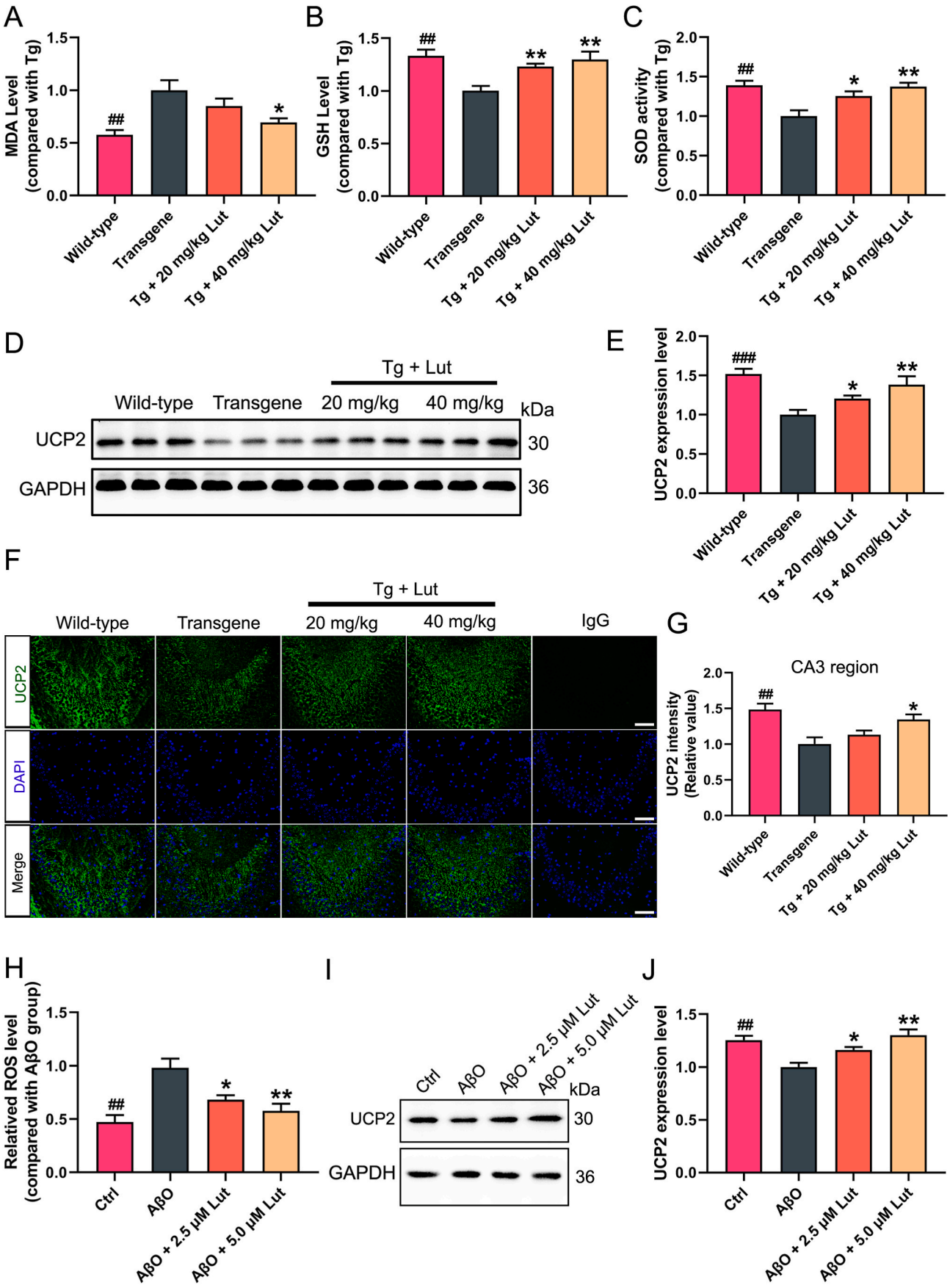

(caption on next page)

Fig. 3. Inhibition of oxidative stress by luteolin in 3×Tg-AD mice and primarily cultured neurons. (A–B) Levels of MDA and GSH in the brain of WT, AD, and Lut-treated AD mice were determined with MDA and GSH assay kits, respectively. **(C)** Activity of SOD in the brain of mice were measured by SOD assay kit. **(D–E)** Representative results of Western blot analysis showed the levels of UCP2 in the brain of mice. Quantification results were normalized against the levels of GAPDH. **(F–G)** Representative immunofluorescent images showed the levels of UCP2 in CA3 region of the hippocampus (Scale bar: 100 μm). Quantitative analysis of fluorescence intensity of UCP2 in this region. As a negative control, rabbit control IgG was used instead of primary antibodies. **(H)** Representative levels of ROS in AβO-induced primary neurons were measured by DCFH-DA fluorescence probe. **(I–J)** Representative results of Western blot analysis showed the levels of UCP2 in Aβ-induced primary neurons. Quantification results were normalized against the levels of GAPDH. #: WT group vs. Tg group or Ctrl group vs. AβO group; *: Tg + Lut group vs. Tg group or AβO + Lut group vs. AβO group. n=6 mice or wells per group; $^{\#\#}P < 0.01$, $^{\#\#\#}P < 0.001$, $^{*}P < 0.05$ and $^{**}P < 0.01$, respectively.

3.5. Luteolin improved mitochondrial dynamics in 3 × Tg-AD mice and primary neurons

Mitochondrial function requires suitable mitochondrial dynamics, which refers to mitochondrial fusion, fission, and translocation inside the cell [38]. To explore the effects of luteolin on mitochondrial dynamics, the classic proteins including dynamin-related protein 1 (Drp1), Fission 1 (Fis1) and mitofusin 2 (Mfn2) required for mitochondrial fusion and fission in hippocampus were determined via Western blot analysis. Compared to WT mice, the levels of Drp1 and Fis1 were enhanced and the level of Mfn2 was diminished in the hippocampus of AD mice. However, treating with luteolin remarkably reversed the pathological alterations of the dynamics-related proteins in the hippocampus of AD mice (Fig. 5A and B). A similar phenomenon was observed in primary neurons. The levels of Drp1 and Fis1 were significantly higher and the level of Mfn2 was obviously lower in Aβ-stimulated primary neurons compared with those in the control group. After treatment of luteolin, the mitochondrial dynamics was recovered, evidenced by the increased Mfn2 level and decreased Drp1 and Fis1 levels in primary neurons (Fig. 5C and D). To summarize, luteolin ameliorated mitochondrial dynamics in AD models.

3.6. Luteolin rescued mitochondrial function

Mitochondrial impairment is an early pathological event in AD. After treatment with luteolin, the morphology of mitochondria in hippocampus of AD mice was observed by TEM. Compared with WT mice, the mitochondria in the hippocampus of AD mice were damaged seriously, shown as fewer, inhomogeneous, swollen and vacuolated. However, treating with luteolin significantly increased the number of mitochondria and improved the defects of mitochondrial structure (Fig. 5E and F). MMP changes with the condition of mitochondria which indicates the health of the neuron [39]. JC-1 is a cationic dye that could aggregate in the mitochondria according to the mitochondrial potential. Under physiological conditions, JC-1 was in the aggregated form and emitted red fluorescence, showing high polarized mitochondria. Once in the pathological condition, JC-1 was in the monomeric form and emitted green fluorescence, indicating low polarized mitochondria. Accordingly, mitochondrial depolarization is determined by the fluorescence intensity ratio of red/green. As displayed in Fig. 5G and H, the ratio of red/green fluorescence in Aβ-stimulated primary neurons was significantly declined by comparing to control neurons, while luteolin treatment notably increased the ratio of red/green fluorescence. These results suggest that luteolin effectively improved the mitochondrial depolarization in AD neuronal cells.

3.7. Luteolin inhibited neuronal apoptosis in 3 × Tg-AD mice and primary neurons

Recent studies have reported that Aβ can directly or indirectly destory the structure and function of mitochondria, leading to the activation of the mitochondrial intrinsic apoptotic pathway [17,20]. To determine whether luteolin could protected against neuronal apoptosis caused by Aβ, mitochondrial pathway apoptosis-related proteins in the hippocampus of AD mice were measured by Western blot analysis. As illustrated in Fig. 6A and B, the expression levels of B-cell lymphoma-2 (bcl-2) was greatly declined and the expression levels of BCL2-related X protein (Bax), cytochrome *c* (CytC), cleaved-caspase9 and cleaved-caspase3 were clearly enhanced in the hippocampi of AD mice by comparing with WT mice. However, luteolin treatment effectively increased the bcl-2 expression levels and decreased Bax, CytC, cleaved-caspase9 and cleaved-caspase3 expression levels. In agreement with Western-blot results, the immunofluorescence staining of brain sections also showed that the degrees of cleaved-caspase3 in CA3 region of hippocmapus of AD mice were much higher than those in WT mice, whereas luteolin treatment markedly reduced the immunoreactive signals of cleaved-caspase3 (Fig. 6C and D).

To further confirm the role of luteolin on neuronal apoptosis induced by Aβ in vitro, the primary neurons were treated with luteolin at concentrationsof 2.5 and 5 μmol/L. The levels of apoptosis-related proteins in cell lysates were analyzed by Western blotting. As expected, luteolin remarkably enhanced the degrees of bcl-2 and suppressed the degrees of Bax, CytC, cleaved-caspase9 and cleaved-caspase3 in Aβ-induced neurons (Fig. 6E and F). Similar results were also illustrated by immunofluorescence staining of MAP2 and cleaved-caspase3 (Fig. 6G and H). Next, TUNEL staining was applied to determine the number of apoptotic neurons. As demonstrated in Fig. 6I and J, the numbers of TUNEL-positive neurons was clearly increased in the Aβ-induced group by comparing with control group, while luteolin treatment clearly reduced the ratio of TUNEL-positive neurons. Collectively, our results indicated luteolin protected against mitochondrial pathway-related apoptosis induced by Aβ in 3 × Tg-AD mice and primary neurons.

3.8. Luteolin enhanced PPARγ expression and activity in 3 × Tg-AD mice and primary neurons

Many studies have demonstrated that PPARγ plays a critial role in neuronal protection [10,36]. To determine whether luteolin could affect the PPARγ expression both in AD mice and primary neurons, the levels of PPARγ were measured by western blot analysis. Compared to WT mice, the expression levels of PPARγ were greatly declined in AD mice, while luteolin treatment significantly enhanced the levels of this protein in the hippocampus of AD mice (Fig. 7A and B). Compared to that in primary hippocampal neurons obtained from newborn WT mice, the PPARγ levels in the primary hippocampal neurons of AD mice obviously decreased, and treatment with 5 μmol/L luteolin significantly restored the level of PPARγ (Fig. 7C and D). In addition, similar results were also illustrated by immunofluorescence assay with double labeling of MAP2 and PPARγ in primary neurons (Fig. 7E–F).

Molecular docking simulation was conducted to investigated the binding mode of luteolin inside the active site of PPARγ protein by using softwares Autodock vina 1.1.2 and Free of Meastro 10.1. The binding affinity of luteolin with PPARγ was calculated theoretically to be −8.9 kcal/mol (mean value), suggesting luteolin had good binding affinity toward the PPARγ receptor. The optimal docking mode and configuration of luteolin with PPARγ were shown in Fig. 8A and B. Docking studies have demonstrated that PPARγ agonists set up a hydrogen bond with the Arg288 and Ser289 residue of PPARγ, and that the hydrophobic effect is critical for binding the agonists with the receptor [40]. Here, the outcomes of molecular docking indicated three hydrogen bonds generated at the Leu340, Leu228 and Arg288 residues between luteolin and PPARγ, suggesting luteolin well interacted with PPARγ, and was therefore a potential agonist for PPARγ activity (Fig. 8C and D). To further explore whether luteolin could directly interact with PPARγ, the binding

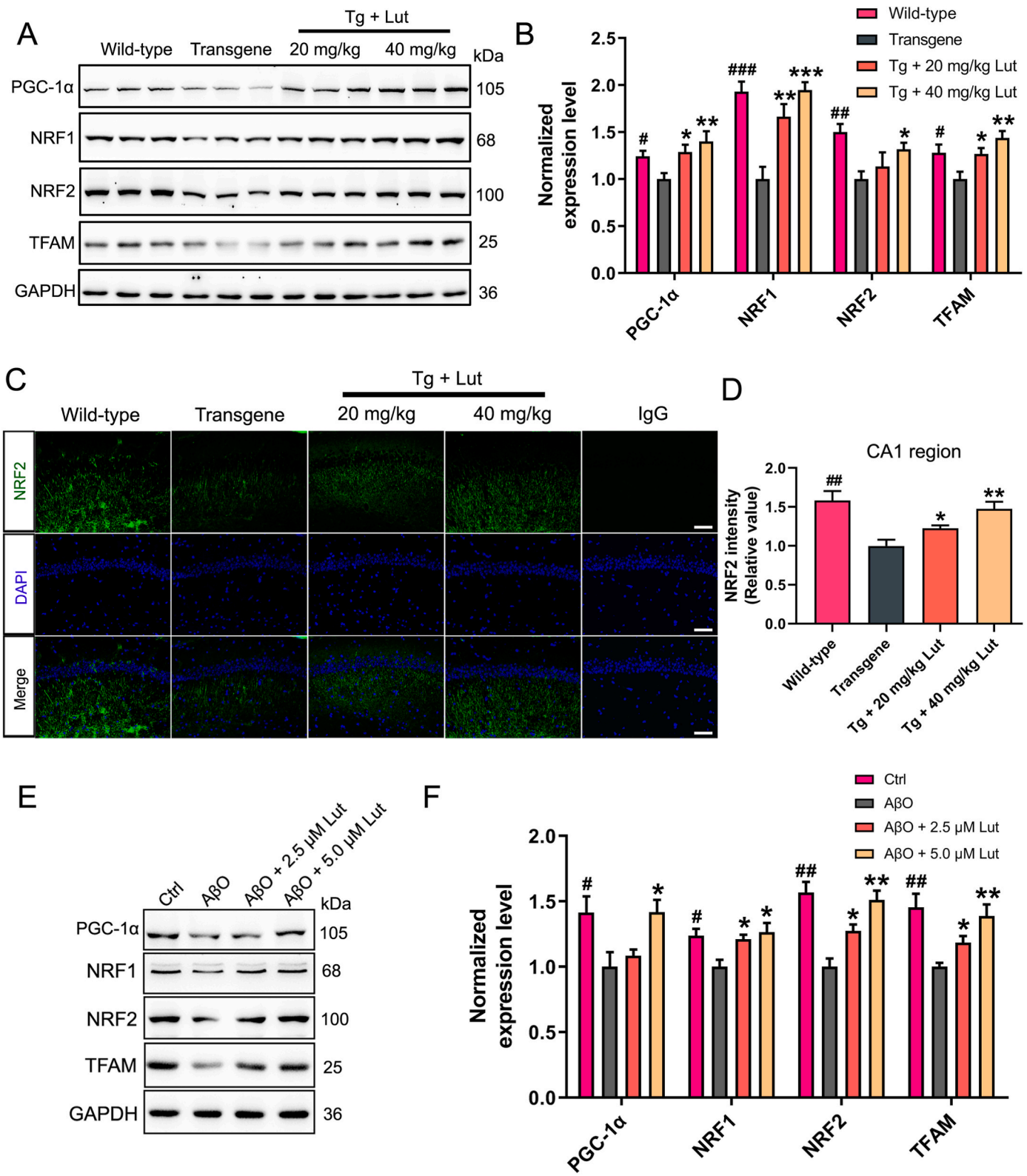

Fig. 4. Enhancement of mitochondrial biogenesis by luteolin in 3×Tg-AD mice and primarily cultured neurons. (A–B) Representative results of Western blot analysis showed the levels of PGC-1α, NRF1, NRF2 and TFAM in the hippocanpus of mice. Quantification results were normalized against the levels of GAPDH. **(C–D)** Representative immunofluorescent images showed the levels of NRF2 in CA1 region of the hippocampus (Scale bar: 100 μm). Quantitative analysis of fluorescence intensity of NRF2 in this region. As a negative control, rabbit control IgG was used instead of primary antibodies. **(E–F)** Representative results of Western blot analysis showed the levels of PGC-1α, NRF1, NRF2 and TFAM in AβO-induced primary neurons. Quantification results were normalized against the levels of GAPDH. #: WT group vs. Tg group or Ctrl group vs. AβO group; *: Tg + Lut group vs. Tg group or AβO + Lut group vs. AβO group. n=6 mice or wells per group; $^{\#}P < 0.05$, $^{\#\#}P < 0.01$, $^{\#\#\#}P < 0.001$, $^{*}P < 0.05$, $^{**}P < 0.01$ and $^{***}P < 0.001$, respectively.

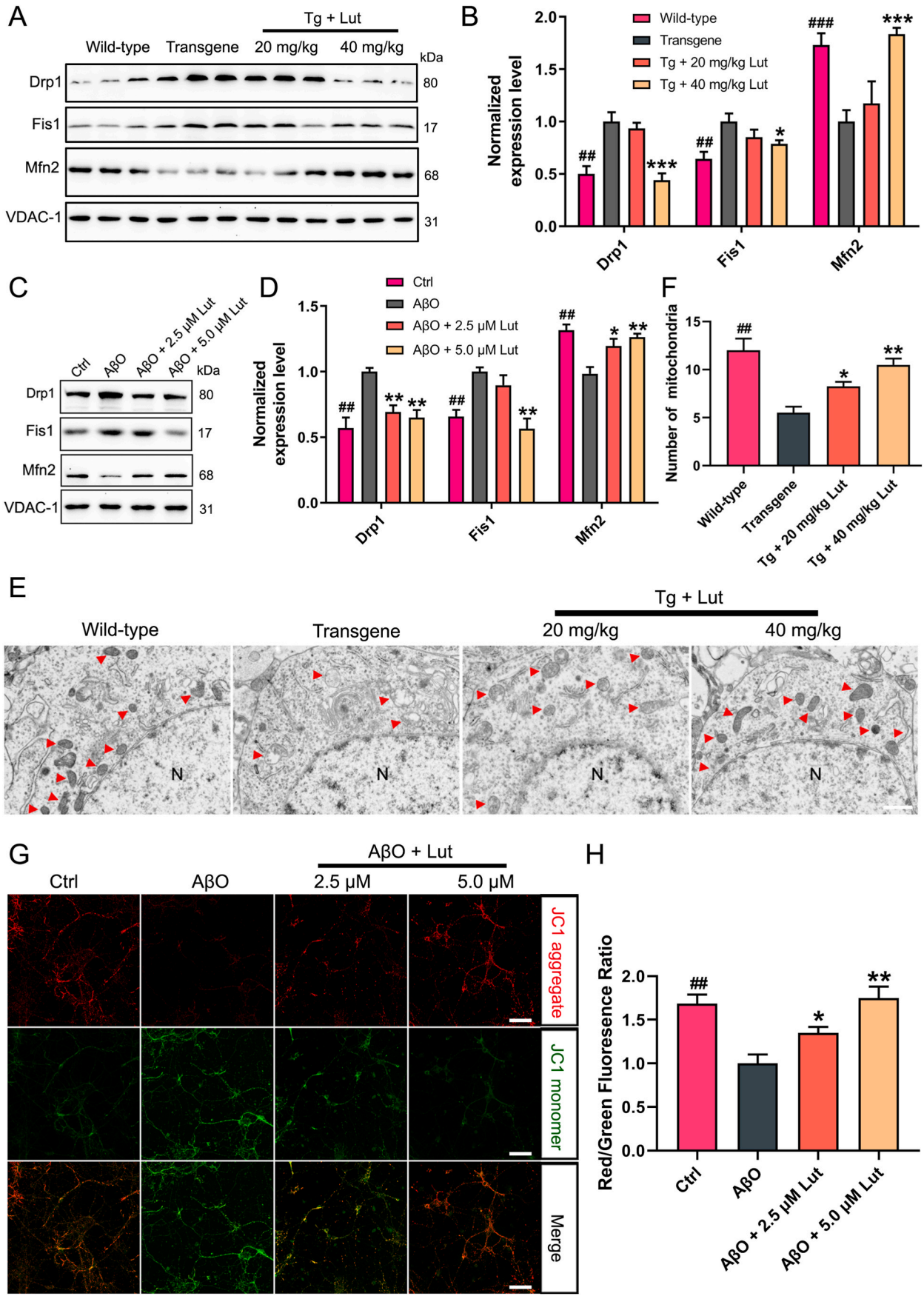

(caption on next page)

Fig. 5. Improvement of mitochondrial dynamics and health by luteolin in 3×Tg-AD mice and primarily cultured neurons. (A–D) Representative results of Western blot analysis showed the levels of Drp1, Fis1 and Mfn2 in the hippocampus of mice and AβO-induced primary neurons, respectively. Quantification results were normalized against the levels of VDAC-1. **(E–F)** Transmission electron microscopic images of mitochondria (red arrows) in the hippocampus of the brain of mice. N, nucleus. The numbers of mitochondria were quantified in equal areas (Scale bar: 10 μm). **(G–H)** Representative images of neurons stained with JC-1 showed the levels of MMP (Scale bar: 50 μm). Red/green fluorescence intensity were quantified. #: WT group vs. Tg group or Ctrl group vs. AβO group; *: Tg + Lut group vs. Tg group or AβO + Lut group vs. AβO group. n=6 mice/wells per group; $^{\#\#}P < 0.01$, $^{\#\#\#}P < 0.001$, $^{*}P < 0.05$, $^{**}P < 0.01$ and $^{***}P < 0.001$, respectively. (For interpretation of color in this figure, the reader is referred to the Web version of this article.)

affinity of luteolin to PPARγ in vitro was detected by Fortebio's Octet RED System and calculated by instrument calculation software. As shown in Fig. 8E, the affinity of luteolin to PPARγ ehanced with the concentration of luteolin and the dissociation constant K_D value was 9.69×10^{-6} M. Taken together, these findings indicated that luteolin could increase the expression level of PPARγ and directly bind to PPARγ.

3.9. Luteolin inhibited Aβ generation, mitochondrial dysfunction and neuronal apoptosis via PPARγ activation

To further elucidate the underlying mechanisms of luteolin in the regulation of Aβ production, oxidative stress, mitochondrial dysfunction and neuronal apoptosis, primary hippocampal neurons were treated with luteolin and GW9662 (a potent PPARγ antagonist), simultaneously. Firstly, the protein levels of PPARγ were measured via Western blot analysis. As expected, the results displayed that GW9662 efficiently impeded the effect of luteolin on increasing the expression level of PPARγ (Supplementary Fig. 3). Secondly, the protein levels of APP, BACE1, $Aβ_{1-42}$ and IDE in the cultured hippocampal neurons were measured by Western blot analysis. As demonstrated in Fig. 9A and B, the addition of GW9662 into the culture medium inhibited the luteolin-induced increase of IDE level and decreases of BACE1 and $Aβ_{1-42}$ levels. Of note, the protein level of APP was not clearly different when GW9662 was added compared to the hippocampal neurons that were treated with luteolin alone. Meanwhile, the expression levels of mitochondrial biogenesis- and dynamics-related proteins were measured in primary hippocampal neurons after treating with Aβ, with or without luteolin and GW9662. As demonstrated in Fig. 9 C–F, the effects of luteolin on improvement of mitochondrial biogenesis and dynamics were negated by GW9662. Next, luteolin was found to ameliorate the oxidative stress in Aβ-treated primary hippocampal neurons, as demonstrated in Fig. 9G–I, while GW9662 also removed the effects of luteolin. Furthermore, the levels of mitochondrial pathway apoptosis-related proteins were also detected. Western blot analyses indicated that inhibition of PPARγ by GW9662 efficiently restored the levels of bcl-2, Bax, CytC, cleaved-caspase9 and cleaved-caspase3 that were changed by luteolin treatment (Fig. 9J and K).

To further verify whether luteolin exerted neuroprotective effect through PPARγ, we silenced the PPARγ in primarily cultured neurons from hippocampus by transfection of PPARγ siRNA. Results of real-time qPCR and Western blot analyses showed that PPARγ siRNA reduced the mRNA and protein levels of PPARγ both in untreated and luteolin-treated primary neurons, confirming that PPARγ was successfully knocked down (Supplementary Fig. 4 and Supplementary Fig. 5). Meanwhile, luteolin-induced mRNA changes in BACE1, IDE, PGC-1α, NRF1, Drp1 and UCP2 were also attenuated by PPARγ siRNA in hippocampal neurons (Supplementary Fig. 6). The expression levels of those proteins, including APP, BACE1, $Aβ_{1-42}$ and IDE in hippocampal neurons, were also analyzed by Western blotting. As shown in Fig. 10A and B, knockdown of PPARγ suppressed the luteolin-induced increase of IDE level and the decreases of BACE1 and $Aβ_{1-42}$ levels, but did not affect the expression of APP. Additionally, mitochondrial biogenesis- and dynamics-related proteins including PGC-1α, NRF1, NRF2, TFAM, Drp1, Fis1 and Mfn2 were determined by Western blot analysis. As expected, knockdown of PPARγ eliminate the effect of luteolin on the expression of these proteins (Fig. 10C-F). The levels of oxidative stress in the hippocampal neurons were also analyzed. According to the results shown in Fig. 10G–I, the increased UCP2 and decreased ROS caused by luteolin were attenuated after PPARγ knockdown. Finally, the levels of apoptosis-associated proteins were explored and the enhanced bcl-2 and reduced Bax, CytC, cleaved-caspase9 and cleaved-caspase3 caused by luteolin were eliminated after PPARγ knockdown (Fig. 10J–K). Collectively, these findings supported the idea that luteolin treatment suppressed the Aβ generation, mitochondrial damage and neuronal apoptosis via a PPARγ-dependent mechanism.

4. Discussion

AD is an unalterable, complex, multifactorial, progressive neurodegenerative disorder characterized by cognitive declines and behavioral changes and is the most common cause of dementia. At present, there are no efficacious therapeutic drugs to slow or stop the progression of this disease. Although four drugs including tacrine, rivastigmine, memantine and donepezil are used clinically to treat AD, they are only able to temporarily improve AD symptoms [41,42]. Recently, the amyloid monoantibody aducanumab (BIIB-037) was granted conditional approval by the US Food and Drug Administration (FDA) for treatment of mild AD. However, the efficacy of aducanumab as a treatment for the cognitive impairment in AD cannot be confirmed by clinical trials with divergent outcomes and the adverse events of aducanumab, including headache, brain microhemorrhages and vasogenic cerebral edema, should not be ignored [43–46]. Thus, it is extremely need for the development of safe and effective drugs to treat AD. Luteolin is a flavonoid compound which can be obtained from different types of herbs. The pharmaceutical roles of luteolin are considered to be linked with its antioxidant potential, anti-tumorigenic effects, anti-inflammatory and neuroprotective activities [30,47]. Previous studies have shown that luteolin can inhibit endoplasmic reticulum stress-dependent neuroinflammation in AD mice and mitigate ROS insult in primary neurons [30,31]. Our current study, for the first time, demonstrated that luteolin was a neuroprotective agent against AD-related accumulation of Aβ, mitochondrial damage and neuronal apoptosis in the brains of 3 × Tg-AD mice. For mechanistic purposes, we used specific PPARγ antagonis (GW9662) and siRNA in primary neurons, which confirmed that luteolin, in a PPARγ-dependent manner, improved Aβ pathology and reduced Aβ-induced neurodegeneration.

As a progressive neurodegenerative brain disease, the main feature of AD besides hyperphosphorylated tau is an accumulation of Aβ. BACE1 appears to be the pivotal rate-limiting enzyme for Aβ production and inhibition or deletion of BACE1 from mice and primary neurons resulted in a reduced levels of Aβ [36,48]. IDE, a ubiquitous zinc-metalloprotease, selectively degrades the monomer of amyloidogenic peptides and contributes to clearance of Aβ [49]. Moreover, elevated level of IDE was tightly associated with the declined level of Aβ in AD [36]. Therefore, down-regulation of BACE1 and up-regulation of IDE levels have been identified as critical strategies for anti-AD therapy [50]. Conforming to these results, the present outcomes showed that the expression levels of several key proteins in the amyloidogenic cascade including APP, BACE1, and $Aβ_{1-42}$ were clearly enhanced, while the expression level of IDE was remarkably declined in the brain of AD mice and primary neurons. As expected, luteolin therapy efficiently increased the level of IDE and reduced the levels of BACE1 and $Aβ_{1-42}$ (Fig. 2). The protein levels of APP showed no remarkable diversity between AD and luteolin-treated group indicating that APP expression was not affected by luteolin. Based on these results, AD pathology can be improved by luteolin through reducing the generation of Aβ via BACE1 inhibition and

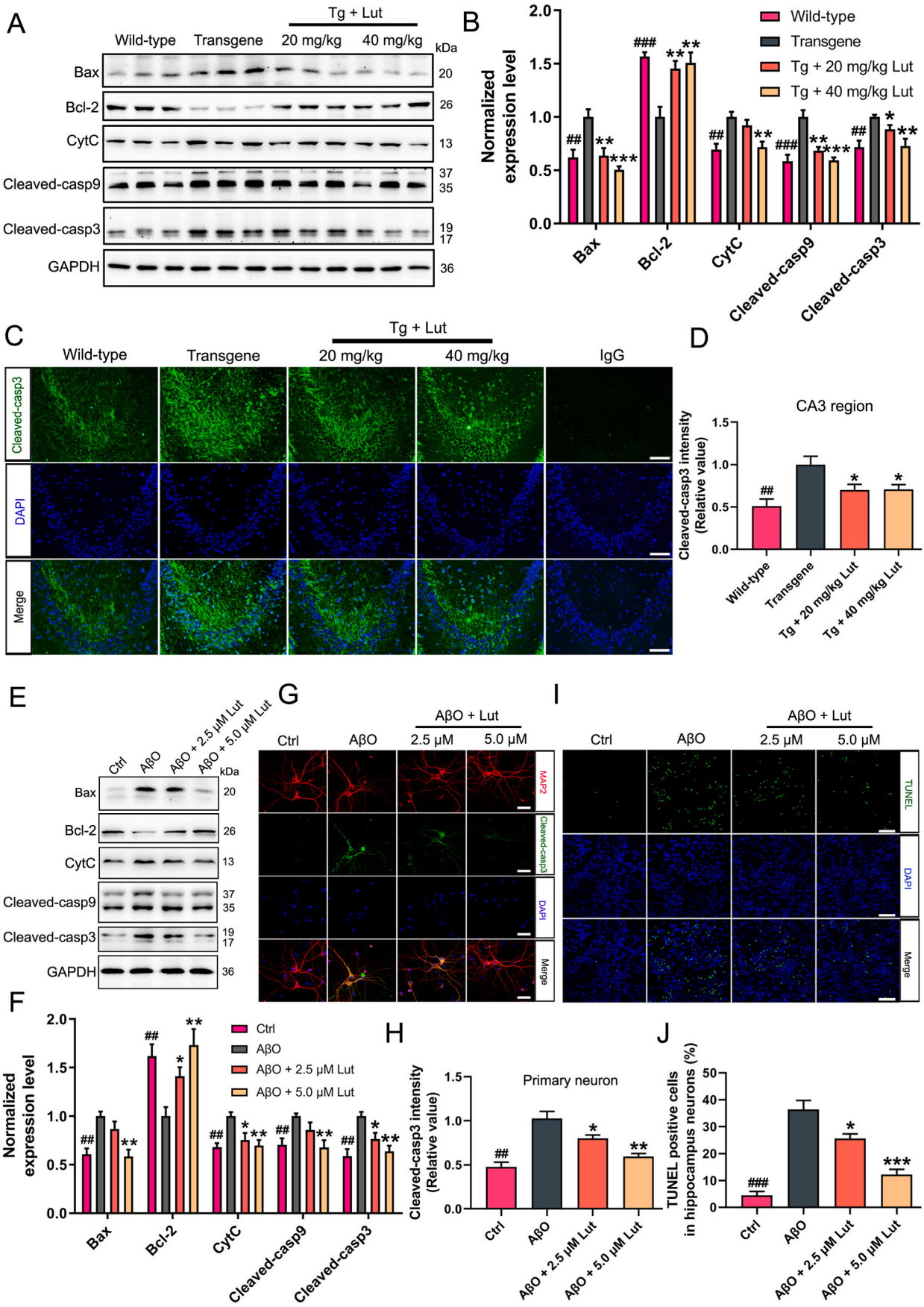

(caption on next page)

Fig. 6. Inhibition of neuronal apoptosis by luteolin in 3×Tg-AD mice and primarily cultured neurons. (A, E) Representative results of Western blot analysis showed the levels of Bax, bcl-2, CytC, cleaved-caspase 9 and cleaved-caspase 3 in the hippocampus of mice and AβO-induced primary neurons, respectively. **(B, F)** Quantification results were normalized against the levels of GAPDH. **(C, G)** Representative immunofluorescent images showed the levels of cleaved-caspase 3 in CA3 region of the hippocampus (Scale bar: 100 μm) and AβO-induced primary neurons (Scale bar: 20 μm). As a negative control, rabbit control IgG was used instead of primary antibodies. **(D, H)** Quantitative analysis of fluorescence intensity of cleaved-caspase 3. **(I, J)** Representative TUNEL staining images of apoptotic neurons displayed the effect of luteolin on AβO-induced primary neurons (Scale bar: 100 μm). The fluorescence intensity of TUNEL staining were quantified. #: WT group vs. Tg group or Ctrl group vs. AβO group; *: Tg + Lut group vs. Tg group or AβO + Lut group vs. AβO group. n=6 mice or wells per group; $^{\#\#}P < 0.01$, $^{\#\#\#}P < 0.001$, $^{*}P < 0.05$, $^{**}P < 0.01$ and $^{***}P < 0.001$, respectively.

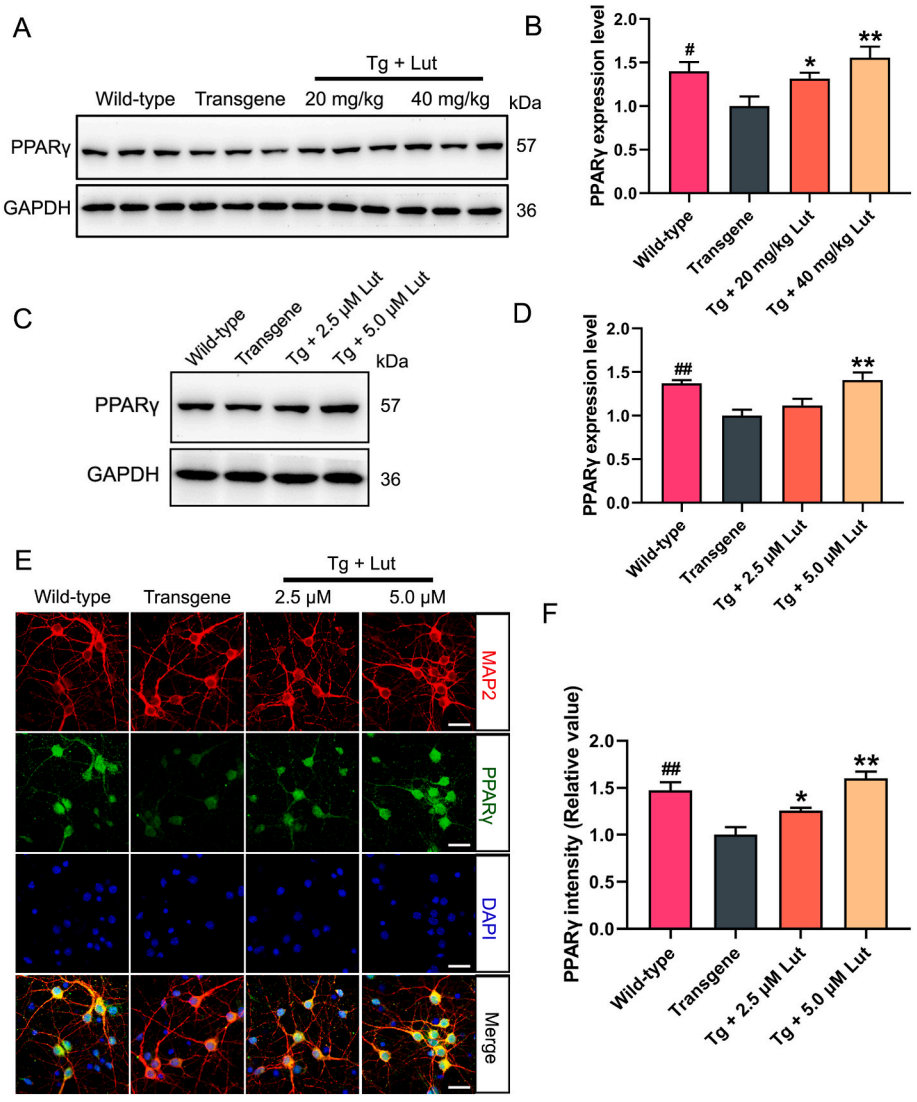

Fig. 7. Increase of PPARγ expression by luteolin in hippocampus of AD mice and primary hippocampal neurons. (A, C) Representative results of Western blot analysis showed the levels of PPARγ in the hippocampus of mice and primary neurons, respectively. **(B, D)** Quantification results were normalized against the levels of GAPDH. **(E, F)** Representative immunofluorescent images showed the levels of PPARγ in primary neurons (Scale bar: 20 μm). Quantitative analysis of fluorescence intensity of PPARγ. #: WT group vs. Tg group; *: Tg + Lut group vs. Tg group. n=6 miceor wells per group; $^{\#}P < 0.05$, $^{\#\#}P < 0.01$, $^{*}P < 0.05$ and $^{**}P < 0.01$, respectively.

accelerating Aβ degradation via IDE elevation.

Oxidative stress, which is closely related to the production and aggregation of Aβ and the phosphorylation and polymerization of tau, acts as a critical factor contributing to the initiation and progression of AD [51]. The degrees of MDA and ROS, whose aberrant production by injured mitochondria results in oxidative stress, were greatly enhanced in the brain of AD mice and AD-related cell line [10,52]. SOD and GSH, two main antioxidants for free radical scavenging, have been used as indicators of lipid peroxidation severity and the degrees of these enzymes are greatly altered by Aβ in AD mice [10,53]. The pharmacological blockade of oxidative stress has been considered as an effective method to stop the pathological progression of AD [54,55]. For example, the resveratrol-loaded neuronal mitochondria-targeted micelles can alleviate cognitive deficits by suppressing oxidative stress in APP/PS1 transgenic mice. In keeping with those reports, our present study also display that the degrees of ROS and MDA was clearly increased, while the level of GSH and the activity of SOD were notably decreased in the brain of 3 × Tg-AD mice and AβO-induced primary neurons. Treatment with luteolin effectively reduced the degrees of MDA and ROS, and enhanced the level of GSH and the activity of SOD, suggesting that luteolin has an inhibitory effect on Aβ-induced oxidative stress. UCP2, a member of the anion carrier family localized in the inner mitochondrial membrane, is widely recognized as an important mediator of ROS production in mitochondria [56]. Recent studies have proven that UCP2 has the protective effect on neurons through the function to regulate the production of reactive oxygen species [57,58] and the level of UCP2 was down-regulated in the AD brains [59]. Consistent with these findings, we verified in the current study that the protein expression level of UCP2

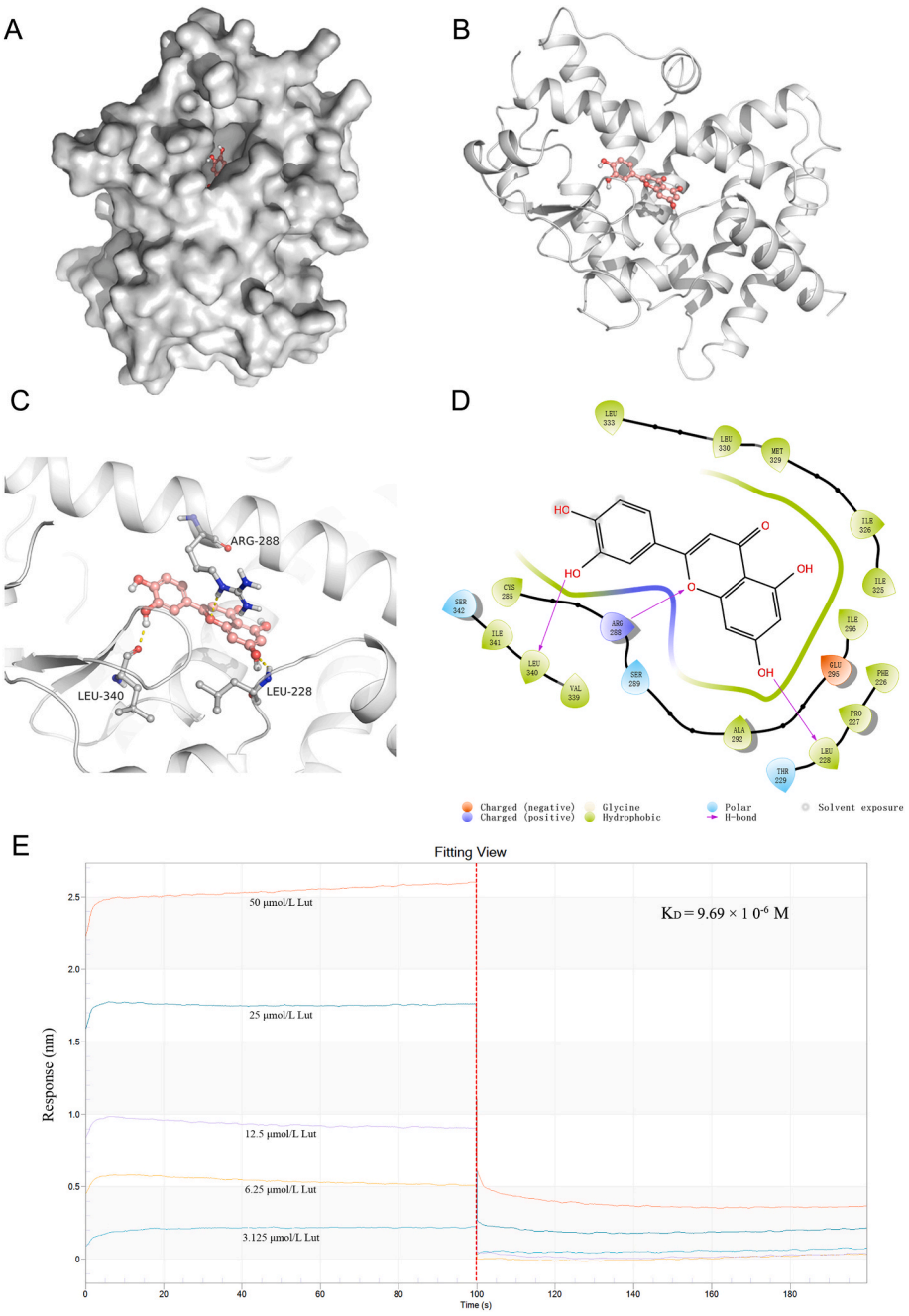

Fig. 8. Direct interaction between **PPARγ** and **luteolin. (A–B)** The docking mode of luteolin with PPARγ protein. **(C)** Luteolin interacts with the ligand-binding domain of PPARγ and forms three hydrogen bonds at the residues Leu340, Leu228 and Arg288, displayed by dashed yellow line. **(D)** The 2D graph showing interactions of luteolin with the residues of PPARγ. The binding features were displayed in different colors, in which the negative charged, positive charged, polar and hydrophobic residues are portrayed as red, deep blue, light blue and green, respectively. **(E)** The binding affinity of luteolin to PPARγ. Left part displays the dissociation curve of luteolin and PPARγ; right part stands for the relationship curve, the concentrations of luteolin adopted for the test were 3.125, 6.25, 12.5, 25, and 50 μM. (For interpretation of the color in this figure, the reader is referred to the Web version of this article.)

was significantly decreased in 3 × Tg-AD mice and Aβ-induced primary neurons, whereas luteolin remarkably enhanced the degree of UCP2. These results indicate that luteolin could supress the oxidative stress via UCP2 elevation (Fig. 3).

Mitochondrial biogenesis plays a crucial role in maintaining mitochondrial health and organismal homeostasis in eukaryotic cells [60]. PGC1α is deemed a main transcription regulator of mitochondrial biogenesis in cells by virtue of its ability to enhance the expression and activity of several pivotal transcription factors [61]. Once being activated via either de-acetylation or phosphorylation, PGC-1α immediately translocates from the cytoplasm into the nucleus to activate downstream NRF1 and NRF2, and subsequently TFAM and mtDNA transcriptional regulators. The activation of this PGC-1α-NRF-TFAM pathway results in synthesis of mitochondrial DNA and proteins as well as generation of new mitochondria [62,63]. Mitochondrial biogenesis disorder is closely linked to the pathogenesis of AD through the PGC-1α-NRF-TFAM pathway, and activation of this signaling pathway stimulates mitochondrial biogenesis and induces beneficial effects on mitochondrial function in AD [64,65]. For instance, ebselen and vascular endothelial growth factor can alleviate the disorder of mitochondrial biogenesis via activating PGC-1α-NRF-TFAM pathway in the brain of AD mice and Aβ-induced SH-SY5Y cells, respectively. Similarly, our work also found that the PGC-1α-NRF-TFAM pathway was activated in 3 × Tg-AD mice and Aβ-induced primary neurons after luteolin treatment, which was responsible for mitochondrial biogenesis. This suggested that luteolin could alleviate the disorder of mitochondrial biogenesis by activating PGC-1α-NRF-TFAM pathway (Fig. 4).

Mitochondrial dynamics, which are involved in mitochondrial fusion and fission, controls mitochondrial function, morphology and intracellular localization. Mitochondrial fusion processes are regulated by three conserved transmembrane GTPases proteins, namely, Mfn1, Mfn2 in the mitochondrial outer membrane and optic atrophy 1 protein (OPA1) in

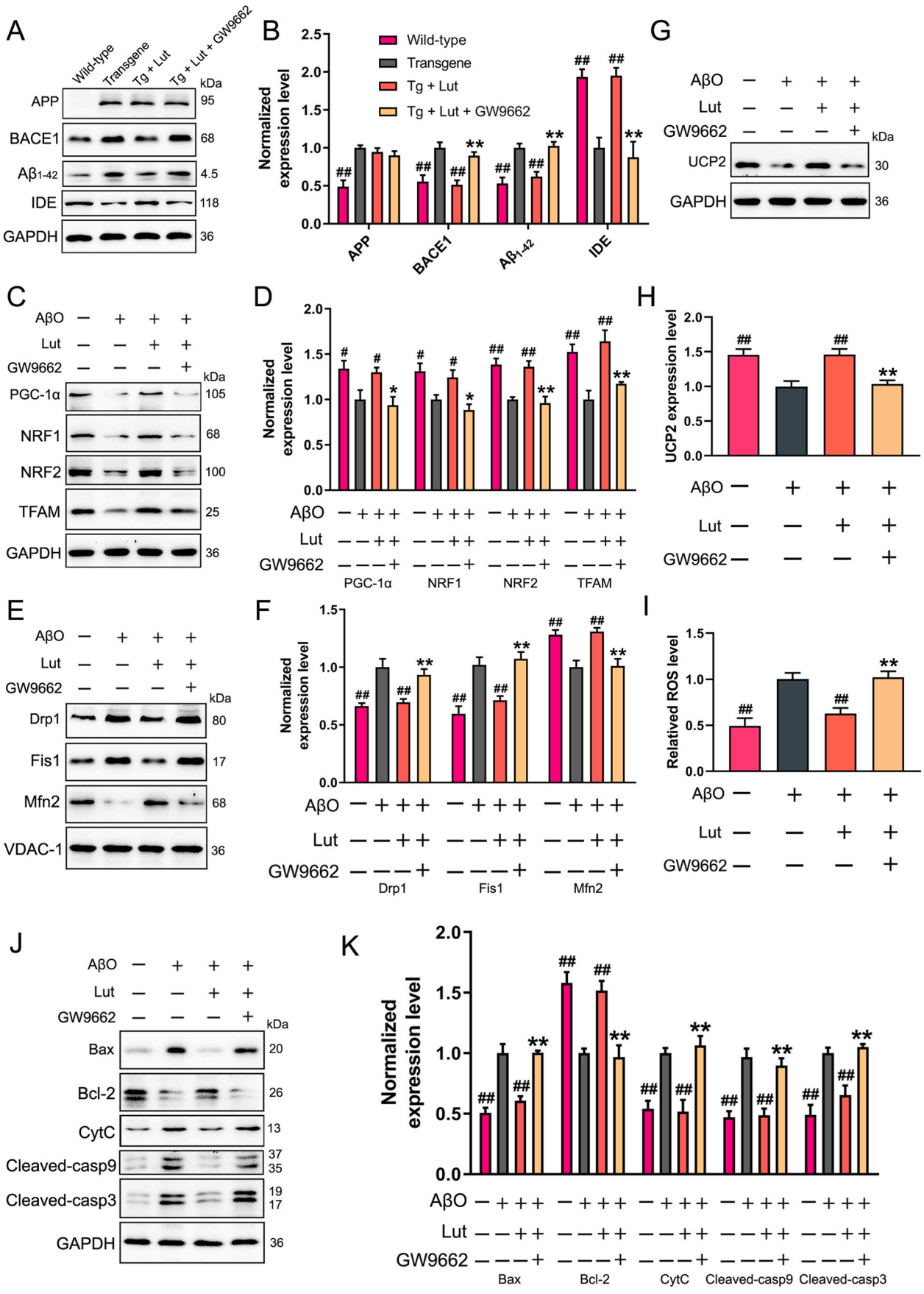

(caption on next page)

Fig. 9. Effects of luteolin on AβO-induced oxidative stress, mitochondrial dysfunction and neuronal apoptosis by activating PPARγ. (A–B) Primary hippocampal neurons were isolated respectively from WT or Tg mice. Neurons from Tg mice were also cultured with 5 μM luteolin and GW9662 for 24 h. Representative results of Western blot analysis showed the levels of APP, BACE1, $A\beta_{1-42}$ and IDE. Quantification results were normalized against the levels of GAPDH. #: WT group or Tg + Lut group vs. Tg group; *: Tg + Lut + GW9662 group vs. Tg + Lut group. n=6 wells per group; $^{\#\#}P < 0.01$ and $^{**}P < 0.01$, respectively. **(C, E, G)** Primary hippocampal neurons isolated from WT mice were co-treated with Aβ oligomer (AβO), luteolin and GW9662 for 24 h. Representative results of Western blot analysis showed the levels of PGC-1α, NRF1, NRF2, TFAM, Drp1, Fis1, Mfn2 and UCP2 in AβO-induced primary neurons. **(D, F, H)** Quantification results were normalized against the levels of GAPDH or VDAC1. **(I)** Representative levels of ROS in AβO-induced primary neurons were measured by DCFH-DA fluorescence probe. **(J–K)** Representative results of Western blot analysis showed the levels of Bax, bcl-2, CytC, cleaved-caspase 9 and cleaved-caspase 3. Quantification results were normalized against the levels of GAPDH. #: untreated or AβO + Lut group vs. AβO group; *: AβO + Lut + GW9662 group vs. AβO + Lut group. n=6 wells per group; $^{\#}P < 0.05$, $^{\#\#}P < 0.01$, $^{*}P < 0.05$ and $^{**}P < 0.01$, respectively.

the intima [66]. This process permits exchange of mtDNA and mitochondria matrix between different mitochondrias, which prefers optimal mitochondrial physiology via diluting mutated mtDNA molecules and saving damaged mitochondria via the obtaintion of critical components from healthy mitochondria [67,68]. In contrast, mitochondrial fission process, regulated by dynamin related protein 1 (Drp1) and fission 1 (Fis1) protein, allows preexisting mitochondria to products a new mitochondria without mtDNA molecules replication. Multiple lines of researches have scientifically proven that the expression levels of Drp1 and Fis1 are enhanced in the brain of AD mice, while the expression levels of OPA1, Mfn1 and Mfn2 are declined [65,69]. Moreover, it has also been demonstrated that reductions in Drp1 expression can reduce Aβ generation, improve mitochondrial dysfunction, maintain mitochondrial dynamics, and increase synaptic activity in AD mice [70,71]. In accordance with these findings, our data in this study confirmed that Drp1 and Fis1 expression were greatly increased, while Mfn2 expression was significantly decreased in the AD models. This phenomenon was obviously reversed by luteolin treatment. Therefore, luteolin could promote mitochondrial fusion via Mfn2 elevation and inhibit mitochondrial fission via Drp1 and Fis1 inhibition. Mitochondrial function, a vital indicator of cell health, can be evaluated by monitoring changes in MMP. It was reported that the number of mitochondria and the level of MMP were decreased in AD models [65]. In addition, increase of mitochondria numbers and MMP levels were considered critical for ameliorating the pathological damage in AD [62]. For example, selenomethionine could improve AD pathologies by inhibiting the decreased number of mitochondria and declined level of MMP in 3 × Tg-AD mice and N2a-SW cells. Similarly, our outcomes also found that luteolin increased mitochondria number, improved the defects of mitochondrial structure, and restored MMP level in the hippocampus of 3 × Tg-AD mice and AβO-induced primary neurons (Fig. 5).

Mitochondria plays a crucial role in a variety of metabolic and apoptotic pathways that control the life and death of cells. Growing evidence has indicated that excessive neuronal apoptosis occurs in AD models which was triggered by a series of causes including cumulative oxidative stress and mitochondrial dysfunction [72]. The mitochondrial pathway apoptosis-related proteins including Bax, bcl-2, CytC, cleaved-caspase9 and cleaved-caspase3 are indicators of the level of neuronal apoptosis in AD [73]. In the present study, an enhanced levels of mitochondrial pathway apoptosis-related proteins were found both in the hippocampus of 3 × Tg-AD mice and Aβ-induced primary neurons, which is consistent with previous findings [74]. As expected, treatment with luteolin reversed the aberrantly expression of Bax, bcl-2, CytC, cleaved-caspase9 and cleaved-caspase3 protein and neuronal apoptosis, which eventually resulted in the improvement of cognitive impairment in AD mice (Fig. 6). Thus, our experimental results demostrated that luteolin targeted oxidative stress and mitochondrial dysfunction induced by Aβ, subsequently suppressed neuronal apoptosis.

As a ubiquitously expressed nuclear factor, PPARγ is well-studied in various types of diseases including neurodegenerative disease, cancer, diabetes and metabolic disease [75,76]. Recent studies have found that PPARγ was closely associated with the initiation and progression of AD, as PPARγ regulates APP processing via inhibiting BACE1 expression and accelerates Aβ degradation via enhancing IDE expression [10,36]. For instance, bis(ethylmaltolato) oxidovanadium (IV), an agonist of PPARγ, can decrease intraneuronal Aβ levels by suppressing the degree of BACE1 and increasing the degree of IDE in the brain of APP/PS1 mice and N2a-SW cells. In contrast, PPARγ block could contribute to the enhance of BACE1 activity, which further promoted the Aβ production process, and finally led to neuronal damage in AD mice [77]. Moreover, it has been found that the level of PPARγ was down-regulated in the AD models [50]. Luteolin exerts protective effects against LPS-induced inflammation by regulating PPARγ in bone marrow derived mast cells [78]. In line with the previous reports, we also found that expression of PPARγ was remarkably decreased in the hippocampus of 3 × Tg-AD mice and primary neurons, while luteolin could interact with PPARγ and restore the degree of PPARγ (Figs. 7 and 8). Applying GW9662 (a PPARγ antagonist) to control PPARγ activity in primary hippocampal neurons, we further confirmed that luteolin reduced the production of Aβ via BACE1 inhibition and IDE-elevated Aβ degradation through a PPARγ-dependent mechanism. Several studies have reported that PPARγ is also involved in mitochondrial function and neuronal apoptosis [79,80]. For example, rosiglitazone can protect hippocampal and dorsal root ganglion neurons against Aβ-induced mitochondrial damage and nerve growth factor deprivation-induced apoptosis by activating PPARγ. Another important issue in this work is to determine whether PPARγ is involved in the roles of luteolin in regulating oxidative stress, mitochondrial damage and neuronal apoptosis in AD. Our experimental outcomes confirmed that GW9662 and PPARγ siRNA could block the antioxidative function of luteolin on mitochondria and apoptotic cascade in primary hippocampal neurons, thus verified the PPARγ-dependent mechanism of luteolin on AβO-induced apoptosis (Figs. 9 and 10). Luteolin was also found in this study to improve mitochondrial structure and biogenesis in AD mouse brains via PPARγ-dependent manner. Briefly, results in this paper confirm the therapeutic effect of luteolin on AD pathology and for the first time reveal its PPARγ-dependent mechanism. These findings help us to understand the target and pathway of some natural products in the treatment of AD. It also helps to fill in the gaps between our knowledge on PPARγ agonists and potential anti-AD drugs, based on the antioxidant property of PPARγ and the oxidative stress-mediated neuropathology of AD. However, a limitation is still present in this study. The effect of luteolin on inflammatory response and its underlying mechanism are not investigated in the current AD model mice or AβO-induced neurons, which is valuable to be detected in the coming study.

This study clearly demonstrated, for the first time, that luteolin administration was able to alleviate the cognitive deficits, anxiety degree and exploring ability in a triple transgenic AD mouse model. Additionally, luteolin could modulate the activity of BACE1 to reduce the generation of Aβ, regulate the level of IDE to promote the clearance of Aβ, and alleviate the impairment of mitochondria to suppress neuronal apoptosis. Moreover, PPARγ takes part in the protective effects of luteolin in AD pathology. The underlying molecular mechanism of luteolin in reducing Aβ levels, restoring mitochondrial damage, inhibiting oxidative stress and improving cognitive functions in AD is summarized in Fig. 11. In conclusion, although further investigation is necessary, our findings provide a theoretical basis for the development of luteolin as a potential candidate for treating AD.

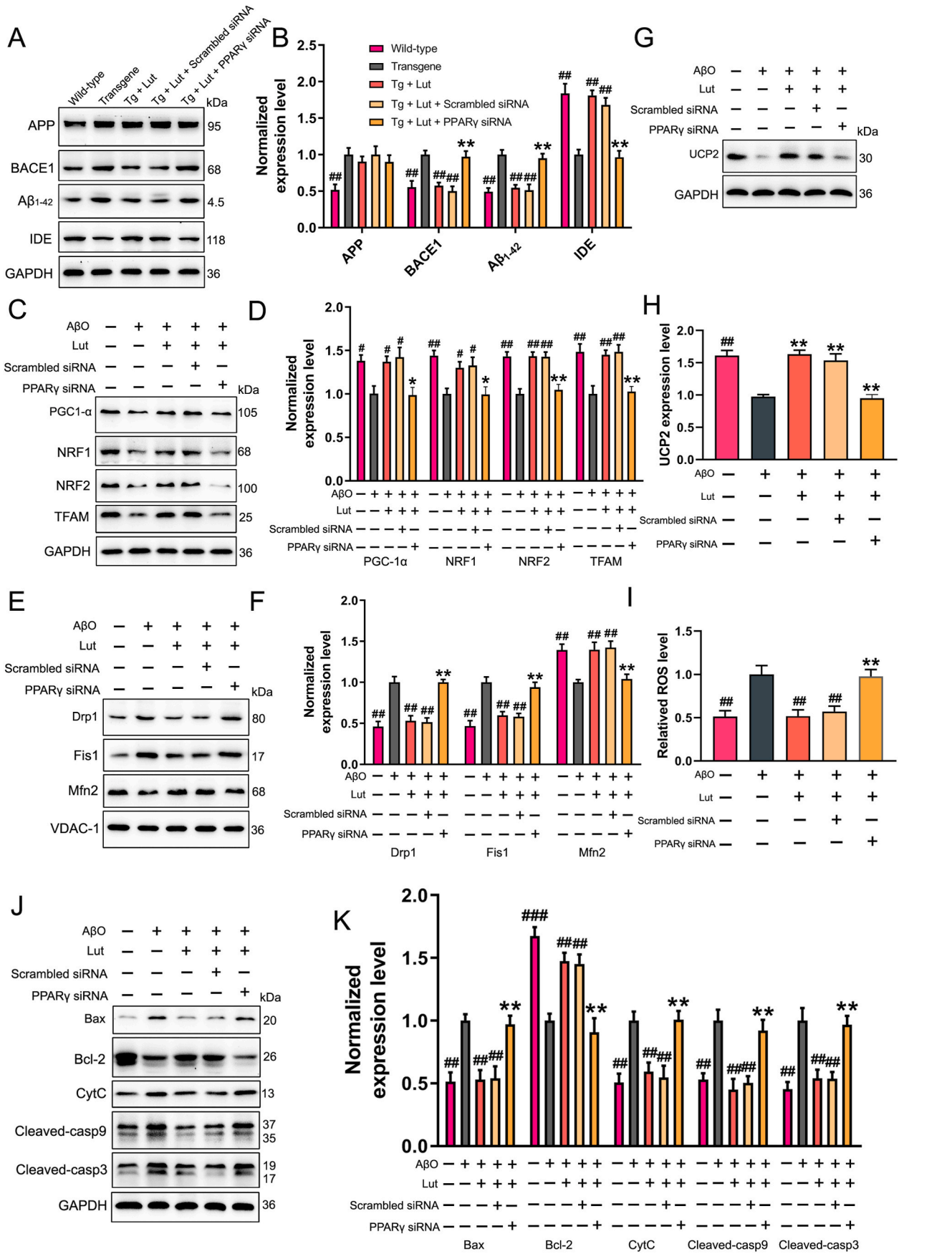

(caption on next page)

Fig. 10. Effects of luteolin on AβO-induced oxidative stress, mitochondrial dysfunction and neuronal apoptosis in PPARγ knockdown neuron. (A–B) Primary hippocampal neurons were isolated respectively from WT or Tg mice. Neurons from Tg mice were cultured with Lut or Lut + scrambled siRNA or Lut + PPARγ siRNA. Representative results of Western blot analysis showed the levels of APP, BACE1, $A\beta_{1-42}$ and IDE. Quantification results were normalized against the levels of GAPDH. #: WT group or Tg + Lut group or Tg + Lut + scrambled siRNA group vs. Tg group; *: Tg + Lut group vs. Tg + Lut + PPARγ siRNA group. n=6 wells per group; $^{\#\#}P < 0.01$ and $^{**}P < 0.01$, respectively. **(C, E, G)** Primary hippocampal neurons isolated from WT mice were co-treated with Aβ oligomer (AβO) and Lut or Lut + scrambled siRNA or Lut + PPARγ siRNA. Representative results of Western blot analysis showed the levels of PGC-1α, NRF1, NRF2, TFAM, Drp1, Fis1, Mfn2 and UCP2 in AβO-induced primary neurons. **(D, F, H)** Quantification results were normalized against the levels of GAPDH or VDAC1. **(I)** Representative levels of ROS in AβO-induced primary neurons were measured by DCFH-DA fluorescence probe. **(J–K)** Representative results of Western blot analysis showed the levels of Bax, bcl-2, CytC, cleaved-caspase 9 and cleaved-caspase 3. Quantification results were normalized against the levels of GAPDH. #: untreated or AβO + Lut group or AβO + Lut + scrambled siRNA group vs. AβO group; *: AβO + Lut group vs. AβO + Lut + PPARγ siRNA group. n=6 wells per group; $^{\#}P < 0.05$, $^{\#\#}P < 0.01$, $^{\#\#\#}P < 0.001$, $^{*}P < 0.05$ and $^{**}P < 0.01$, respectively.

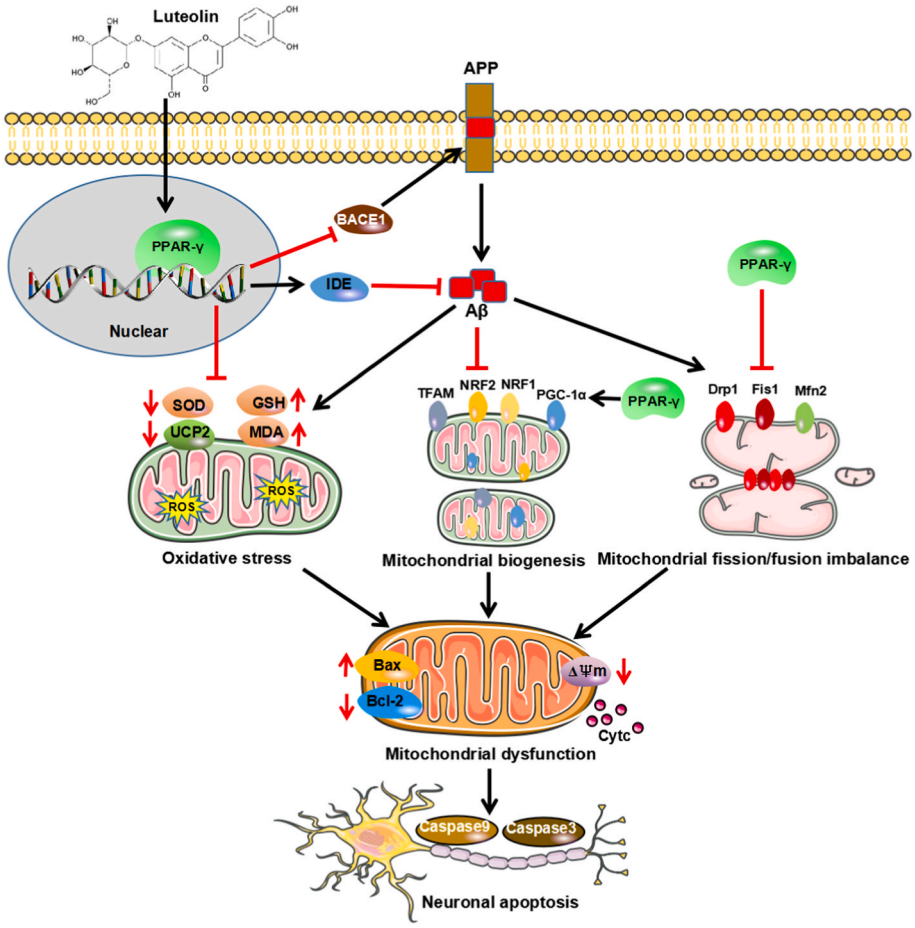

Fig. 11. Proposed mechanism for the protective effect of luteolin on Aβ-induced neuronal apoptosis in AD. Luteolin improved cognitive impairments via inhibiting Aβ production, promoting Aβ degradation, and suppressing mitochondrial dysfunction-induced neuronal apoptosis through a PPARγ-dependent pathway.

Funding information

This study was financially supported by grants from the Shenzhen Science and Technology Innovation Commission (JCYJ20200109110001818), the Shenzhen-Hong Kong Institute of brain Science-Shenzhen Fundamental Research institutions (No. 2023SHIBS0003).

Authors' contributions

QL, and ZJH conceived and designed the project. XQL and ZW conducted the in vitro experiments. ZJH, YQC and XQL performed the cellular experiments. NL and SXH helped in data analysis. JC and SYC contributed in interpreting the results. QL, ZJH and JC co-wrote the manuscript. All authors reviewed and concurred with the final manuscript.

Declaration of competing interest

The authors declare that they have no competing interests.

Data availability

Data will be made available on request.

Acknowledgement

We would like to thank the Central Research Facilities of College of Life Sciences and Oceanography of Shenzhen University for the using of laser scanning confocal microscope (LSM 710, ZEISS, Ger-many) and Testing Center of Shenzhen University for the using of Uitra-high resolution confocal microscopy (LSM 880, ZEISS, Germany).

Appendix A. Supplementary data

Supplementary data to this article can be found online at https://doi.org/10.1016/j.redox.2023.102848.

References

[1] 2021 Alzheimer's disease facts and figures, Alzheimers Dement 17 (2021) 327–406.
[2] S. Jett, N. Malviya, E. Schelbaum, G. Jang, E. Jahan, K. Clancy, et al., Endogenous and exogenous estrogen exposures: how women's reproductive health can drive brain aging and inform Alzheimer's prevention, Front. Aging Neurosci. 14 (2022), 831807.
[3] B. Klimova, P. Maresova, K. Kuca, Non-pharmacological approaches to the prevention and treatment of Alzheimer's disease with respect to the rising treatment costs, Curr. Alzheimer Res. 13 (2016) 1249–1258.
[4] R.E. Tanzi, R.D. Moir, S.L. Wagner, Clearance of Alzheimer's Abeta peptide: the many roads to perdition, Neuron 43 (2004) 605–608.
[5] D.J. Yuan, G. Yang, W. Wu, Q.F. Li, D.E. Xu, M. Ntim, et al., Reducing Nav1.6 expression attenuates the pathogenesis of Alzheimer's disease by suppressing BACE1 transcription, Aging Cell 21 (2022), e13593.
[6] Y. Zhou, F. Zhu, Y. Liu, M. Zheng, Y. Wang, D. Zhang, et al., Blood-brain barrier-penetrating siRNA nanomedicine for Alzheimer's disease therapy, Sci. Adv. 6 (2020).
[7] G. Bahn, J.S. Park, U.J. Yun, Y.J. Lee, Y. Choi, J.S. Park, et al., NRF2/ARE pathway negatively regulates BACE1 expression and ameliorates cognitive deficits in mouse Alzheimer's models, Proc. Natl. Acad. Sci. U.S.A. 116 (2019) 12516–12523.
[8] A.A. Lauer, J. Mett, D. Janitschke, A. Thiel, C.P. Stahlmann, C.M. Bachmann, et al., Regulatory feedback cycle of the insulin-degrading enzyme and the amyloid precursor protein intracellular domain: implications for Alzheimer's disease, Aging Cell 19 (2020), e13264.
[9] W. Farris, S. Mansourian, M.A. Leissring, E.A. Eckman, L. Bertram, C.B. Eckman, et al., Partial loss-of-function mutations in insulin-degrading enzyme that induce diabetes also impair degradation of amyloid beta-protein, Am. J. Pathol. 164 (2004) 1425–1434.
[10] Z. He, X. Li, Z. Wang, S. Tu, J. Feng, X. Du, et al., Esculentoside A alleviates cognitive deficits and amyloid pathology through peroxisome proliferator-activated receptor γ-dependent mechanism in an Alzheimer's disease model, Phytomedicine 98 (2022), 153956.
[11] S.J. Shin, S.G. Jeon, J.I. Kim, Y.O. Jeong, S. Kim, Y.H. Park, et al., Red ginseng attenuates aβ-induced mitochondrial dysfunction and aβ-mediated pathology in an animal model of alzheimer's disease, Int. J. Mol. Sci. 20 (2019).
[12] M.T. Lin, M.F. Beal, Mitochondrial dysfunction and oxidative stress in neurodegenerative diseases, Nature 443 (2006) 787–795.
[13] T.J. Pucadyil, J.E. Chipuk, Y. Liu, L. O'Neill, Q. Chen, The multifaceted roles of mitochondria, Mol. Cell 83 (2023) 819–823.
[14] P.H. Reddy, S. McWeeney, B.S. Park, M. Manczak, R.V. Gutala, D. Partovi, et al., Gene expression profiles of transcripts in amyloid precursor protein transgenic mice: up-regulation of mitochondrial metabolism and apoptotic genes is an early cellular change in Alzheimer's disease, Hum. Mol. Genet. 13 (2004) 1225–1240.
[15] W. Wang, F. Zhao, X. Ma, G. Perry, X. Zhu, Mitochondria dysfunction in the pathogenesis of Alzheimer's disease: recent advances, Mol. Neurodegener. 15 (2020) 30.
[16] X. Yao, J. Zhang, Y. Lu, Y. Deng, R. Zhao, S. Xiao, Myricetin restores aβ-induced mitochondrial impairments in N2a-SW cells, ACS Chem. Neurosci. 13 (2022) 454–463.
[17] K. Leuner, W.E. Müller, A.S. Reichert, From mitochondrial dysfunction to amyloid beta formation: novel insights into the pathogenesis of Alzheimer's disease, Mol. Neurobiol. 46 (2012) 186–193.
[18] J. Zhao, L. Yu, X. Xue, Y. Xu, T. Huang, D. Xu, et al., Diminished α7 nicotinic acetylcholine receptor (α7nAChR) rescues amyloid-β induced atrial remodeling by oxi-CaMKII/MAPK/AP-1 axis-mediated mitochondrial oxidative stress, Redox Biol. 59 (2023), 102594.
[19] L. Yu, S. Wang, X. Chen, H. Yang, X. Li, Y. Xu, et al., Orientin alleviates cognitive deficits and oxidative stress in Aβ1-42-induced mouse model of Alzheimer's disease, Life Sci. 121 (2015) 104–109.
[20] G. Jia, Z. Diao, Y. Liu, C. Sun, C. Wang, Neural stem cell-conditioned medium ameliorates Aβ25-35-induced damage in SH-SY5Y cells by protecting mitochondrial function, Bosn. J. Basic Med. Sci. 21 (2021) 179–186.
[21] S.P. Bapat, C. Whitty, C.T. Mowery, Y. Liang, A. Yoo, Z. Jiang, et al., Obesity alters pathology and treatment response in inflammatory disease, Nature 604 (2022) 337–342.
[22] S. Virtue, K. Petkevicius, J.M. Moreno-Navarrete, B. Jenkins, D. Hart, M. Dale, et al., Peroxisome proliferator-activated receptor γ2 controls the rate of adipose tissue lipid storage and determines metabolic flexibility, Cell Rep. 24 (2018) 2005, 12.e7.
[23] G. Cao, P. Su, S. Zhang, L. Guo, H. Zhang, Y. Liang, et al., Ginsenoside Re reduces Aβ production by activating PPARγ to inhibit BACE1 in N2a/APP695 cells, Eur. J. Pharmacol. 793 (2016) 101–108.
[24] N. Lin, L.M. Chen, X.D. Pan, Y.G. Zhu, J. Zhang, Y.Q. Shi, et al., Tripchlorolide attenuates β-amyloid generation via suppressing PPARγ-regulated BACE1 activity in N2a/APP695 cells, Mol. Neurobiol. 53 (2016) 6397–6406.
[25] Z. Li, X. Meng, G. Ma, W. Liu, W. Li, Q. Cai, et al., Increasing brain glucose metabolism by ligustrazine piperazine ameliorates cognitive deficits through PPARγ-dependent enhancement of mitophagy in APP/PS1 mice, Alzheimer's Res. Ther. 14 (2022) 150.
[26] S. Jamwal, J.K. Blackburn, J.D. Elsworth, PPARγ/PGC1α signaling as a potential therapeutic target for mitochondrial biogenesis in neurodegenerative disorders, Pharmacol. Ther. 219 (2021), 107705.
[27] M.C. Chiang, Y. Chern, R.N. Huang, PPARgamma rescue of the mitochondrial dysfunction in Huntington's disease, Neurobiol. Dis. 45 (2012) 322–328.
[28] J.M. Zolezzi, C. Silva-Alvarez, D. Ordenes, J.A. Godoy, F.J. Carvajal, M.J. Santos, et al., Peroxisome proliferator-activated receptor (PPAR) γ and PPARα agonists modulate mitochondrial fusion-fission dynamics: relevance to reactive oxygen species (ROS)-related neurodegenerative disorders? PLoS One 8 (2013), e64019.
[29] S.G. Jeon, E.J. Song, D. Lee, J. Park, Y. Nam, J.I. Kim, et al., Traditional oriental medicines and alzheimer's disease, Aging Dis 10 (2019) 307–328.
[30] J.J. Kou, J.Z. Shi, Y.Y. He, J.J. Hao, H.Y. Zhang, D.M. Luo, et al., Luteolin alleviates cognitive impairment in Alzheimer's disease mouse model via inhibiting endoplasmic reticulum stress-dependent neuroinflammation, Acta Pharmacol. Sin. 43 (2022) 840–849.
[31] G. Zhao, C. Yao-Yue, G.W. Qin, L.H. Guo, Luteolin from Purple Perilla mitigates ROS insult particularly in primary neurons, Neurobiol. Aging 33 (2012) 176–186.
[32] S. Ahmad, M.H. Jo, M. Ikram, A. Khan, M.O. Kim, Deciphering the potential neuroprotective effects of luteolin against aβ(1)-(42)-induced Alzheimer's disease, Int. J. Mol. Sci. (2021) 22.
[33] L. Li, G. Pan, R. Fan, D. Li, L. Guo, L. Ma, et al., Luteolin alleviates inflammation and autophagy of hippocampus induced by cerebral ischemia/reperfusion by activating PPAR gamma in rats, BMC Complement Med Ther 22 (2022) 176.
[34] T. Boeing, S. Speca, P. de Souza, A.M. Mena, B. Bertin, P. Desreumax, et al., The PPARγ-dependent effect of flavonoid luteolin against damage induced by the chemotherapeutic irinotecan in human intestinal cells, Chem. Biol. Interact. 351 (2022), 109712.
[35] Z. He, H. Zhang, X. Li, S. Tu, Z. Wang, S. Han, et al., The protective effects of Esculentoside A through AMPK in the triple transgenic mouse model of Alzheimer's disease, Phytomedicine 109 (2023), 154555.
[36] Z. He, S. Han, H. Zhu, X. Hu, X. Li, C. Hou, et al., The protective effect of vanadium on cognitive impairment and the neuropathology of Alzheimer's disease in APPSwe/PS1dE9 mice, Front. Mol. Neurosci. 13 (2020) 21.
[37] F. de Bilbao, D. Arsenijevic, P. Vallet, O.P. Hjelle, O.P. Ottersen, C. Bouras, et al., Resistance to cerebral ischemic injury in UCP2 knockout mice: evidence for a role of UCP2 as a regulator of mitochondrial glutathione levels, J. Neurochem. 89 (2004) 1283–1292.
[38] B. DuBoff, M. Feany, J. Götz, Why size matters - balancing mitochondrial dynamics in Alzheimer's disease, Trends Neurosci. 36 (2013) 325–335.
[39] R. Suzuki, K. Hotta, K. Oka, Transitional correlation between inner-membrane potential and ATP levels of neuronal mitochondria, Sci. Rep. 8 (2018) 2993.
[40] J.B. Bruning, M.J. Chalmers, S. Prasad, S.A. Busby, T.M. Kamenecka, Y. He, et al., Partial agonists activate PPARgamma using a helix 12 independent mechanism, Structure 15 (2007) 1258–1271.
[41] R. Briggs, S.P. Kennelly, D. O'Neill, Drug treatments in Alzheimer's disease, Clin. Med. 16 (2016) 247–253.
[42] H. Ma, Y. Dong, Y. Chu, Y. Guo, L. Li, The mechanisms of ferroptosis and its role in alzheimer's disease, Front. Mol. Biosci. 9 (2022), 965064.
[43] D.S. Knopman, D.T. Jones, M.D. Greicius, Failure to demonstrate efficacy of aducanumab: An analysis of the EMERGE and ENGAGE trials as reported by Biogen, December 2019, Alzheimers Dement 17 (2021) 696–701.
[44] S. Salloway, S. Chalkias, F. Barkhof, P. Burkett, J. Barakos, D. Purcell, et al., Amyloid-related imaging abnormalities in 2 phase 3 studies evaluating aducanumab in patients with early Alzheimer disease, JAMA Neurol. 79 (2022) 13–21.
[45] M. Kurkinen, L. Tran, Aduhelm: the best hope for Alzheimer's disease patients or the worst decision the FDA has ever made? J Alzheimers Dis 84 (2021) 969–971.
[46] H. Fillit, A. Green, Aducanumab and the FDA - where are we now? Nat. Rev. Neurol. 17 (2021) 129–130.
[47] D. Kempuraj, R. Thangavel, D.D. Kempuraj, M.E. Ahmed, G.P. Selvakumar, S. P. Raikwar, et al., Neuroprotective effects of flavone luteolin in neuroinflammation and neurotrauma, Biofactors 47 (2021) 190–197.
[48] N. Singh, B. Das, J. Zhou, X. Hu, R. Yan, Targeted BACE-1 inhibition in microglia enhances amyloid clearance and improved cognitive performance, Sci. Adv. 8 (2022), eabo3610.
[49] L.A. McCord, W.G. Liang, E. Dowdell, V. Kalas, R.J. Hoey, A. Koide, et al., Conformational states and recognition of amyloidogenic peptides of human insulin-degrading enzyme, Proc. Natl. Acad. Sci. U.S.A. 110 (2013) 13827–13832.
[50] Z. He, S. Han, C. Wu, L. Liu, H. Zhu, A. Liu, et al., Bis(ethylmaltolato) oxidovanadium(iv) inhibited the pathogenesis of Alzheimer's disease in triple transgenic model mice, Metallomics 12 (2020) 474–490.
[51] D.A. Butterfield, Perspectives on oxidative stress in alzheimer's disease and predictions of future research emphases, J Alzheimers Dis 64 (2018) S469, s79.
[52] M.D. Pandareesh, V. Chauhan, A. Chauhan, Walnut supplementation in the diet reduces oxidative damage and improves antioxidant status in transgenic mouse model of Alzheimer's disease, J Alzheimers Dis 64 (2018) 1295–1305.
[53] Q. Li, J. Wang, Y. Li, X. Xu, Neuroprotective effects of salidroside administration in a mouse model of Alzheimer's disease, Mol. Med. Rep. 17 (2018) 7287–7292.
[54] P. Yang, D. Sheng, Q. Guo, P. Wang, S. Xu, K. Qian, et al., Neuronal mitochondria-targeted micelles relieving oxidative stress for delayed progression of Alzheimer's disease, Biomaterials 238 (2020), 119844.
[55] Y. Xie, Q. Liu, L. Zheng, B. Wang, X. Qu, J. Ni, et al., Se-methylselenocysteine ameliorates neuropathology and cognitive deficits by attenuating oxidative stress

and metal dyshomeostasis in alzheimer model mice, Mol. Nutr. Food Res. 62 (2018), e1800107.
[56] K.S. Echtay, E. Winkler, K. Frischmuth, M. Klingenberg, Uncoupling proteins 2 and 3 are highly active H(+) transporters and highly nucleotide sensitive when activated by coenzyme Q (ubiquinone), Proc. Natl. Acad. Sci. U.S.A. 98 (2001) 1416–1421.
[57] M. Zhang, L. Wang, D. Wen, C. Ren, S. Chen, Z. Zhang, et al., Neuroprotection of retinal cells by Caffeic Acid Phenylethyl Ester(CAPE) is mediated by mitochondrial uncoupling protein UCP2, Neurochem. Int. 151 (2021), 105214.
[58] J. Huang, W. Liu, D.M. Doycheva, M. Gamdzyk, W. Lu, J. Tang, et al., Ghrelin attenuates oxidative stress and neuronal apoptosis via GHSR-1α/AMPK/Sirt1/PGC-1α/UCP2 pathway in a rat model of neonatal HIE, Free Radic. Biol. Med. 141 (2019) 322–337.
[59] R. Thangavel, D. Kempuraj, S. Zaheer, S. Raikwar, M.E. Ahmed, G.P. Selvakumar, et al., Glia maturation factor and mitochondrial uncoupling proteins 2 and 4 expression in the temporal cortex of Alzheimer's disease brain, Front. Aging Neurosci. 9 (2017) 150.
[60] V.N. Kotiadis, M.R. Duchen, L.D. Osellame, Mitochondrial quality control and communications with the nucleus are important in maintaining mitochondrial function and cell health, Biochim. Biophys. Acta 1840 (2014) 1254–1265.
[61] A.P. Gureev, E.A. Shaforostova, V.N. Popov, Regulation of mitochondrial biogenesis as a way for active longevity: interaction between the Nrf2 and PGC-1α signaling pathways, Front. Genet. 10 (2019) 435.
[62] C. Chen, Y. Chen, Z.H. Zhang, S.Z. Jia, Y.B. Chen, S.L. Huang, et al., Selenomethionine improves mitochondrial function by upregulating mitochondrial selenoprotein in a model of Alzheimer's disease, Front. Aging Neurosci. 13 (2021), 750921.
[63] P. Venditti, S. Di Meo, The role of reactive oxygen species in the life cycle of the mitochondrion, Int. J. Mol. Sci. 21 (2020).
[64] C.F. Wang, C.Y. Song, X. Wang, L.Y. Huang, M. Ding, H. Yang, et al., Protective effects of melatonin on mitochondrial biogenesis and mitochondrial structure and function in the HEK293-APPswe cell model of Alzheimer's disease, Eur. Rev. Med. Pharmacol. Sci. 23 (2019) 3542–3550.
[65] X. Li, Q. Shi, H. Xu, Y. Xiong, C. Wang, L. Le, et al., Ebselen interferes with Alzheimer's disease by regulating mitochondrial function, Antioxidants 11 (2022).
[66] T. Rodrigues, L.S. Ferraz, Therapeutic potential of targeting mitochondrial dynamics in cancer, Biochem. Pharmacol. 182 (2020), 114282.
[67] R.J. Youle, A.M. van der Bliek, Mitochondrial fission, fusion, and stress, Science 337 (2012) 1062–1065.
[68] A. Zorzano, M. Claret, Implications of mitochondrial dynamics on neurodegeneration and on hypothalamic dysfunction, Front. Aging Neurosci. 7 (2015) 101.
[69] R. Kandimalla, M. Manczak, X. Yin, R. Wang, P.H. Reddy, Hippocampal phosphorylated tau induced cognitive decline, dendritic spine loss and mitochondrial abnormalities in a mouse model of Alzheimer's disease, Hum. Mol. Genet. 27 (2018) 30–40.
[70] S.H. Baek, S.J. Park, J.I. Jeong, S.H. Kim, J. Han, J.W. Kyung, et al., Inhibition of Drp1 ameliorates synaptic depression, Aβ deposition, and cognitive impairment in an Alzheimer's disease model, J. Neurosci. 37 (2017) 5099–5110.
[71] M. Manczak, R. Kandimalla, D. Fry, H. Sesaki, P.H. Reddy, Protective effects of reduced dynamin-related protein 1 against amyloid beta-induced mitochondrial dysfunction and synaptic damage in Alzheimer's disease, Hum. Mol. Genet. 25 (2016) 5148–5166.
[72] M.I. Islam, M.G. Sharoar, E.K. Ryu, I.S. Park, Limited activation of the intrinsic apoptotic pathway plays a main role in amyloid-β-induced apoptosis without eliciting the activation of the extrinsic apoptotic pathway, Int. J. Mol. Med. 40 (2017) 1971–1982.
[73] N. Jin, H. Zhu, X. Liang, W. Huang, Q. Xie, P. Xiao, et al., Sodium selenate activated Wnt/β-catenin signaling and repressed amyloid-β formation in a triple transgenic mouse model of Alzheimer's disease, Exp. Neurol. 297 (2017) 36–49.
[74] Q.Q. Fu, L. Wei, J. Sierra, J.Z. Cheng, M.T. Moreno-Flores, H. You, et al., Olfactory ensheathing cell-conditioned medium reverts aβ(25-35)-induced oxidative damage in SH-SY5Y cells by modulating the mitochondria-mediated apoptotic pathway, Cell. Mol. Neurobiol. 37 (2017) 1043–1054.
[75] L. Xu, X. Ma, N. Verma, L. Perie, J. Pendse, S. Shamloo, et al., PPARγ agonists delay age-associated metabolic disease and extend longevity, Aging Cell 19 (2020), e13267.
[76] Z. Ning, X. Guo, X. Liu, C. Lu, A. Wang, X. Wang, et al., USP22 regulates lipidome accumulation by stabilizing PPARγ in hepatocellular carcinoma, Nat. Commun. 13 (2022) 2187.
[77] L. Yan, Y. Deng, J. Gao, Y. Liu, F. Li, J. Shi, et al., Icariside II effectively reduces spatial learning and memory impairments in Alzheimer's disease model mice targeting beta-amyloid production, Front. Pharmacol. 8 (2017) 106.
[78] N. Xu, L. Zhang, J. Dong, X. Zhang, Y.G. Chen, B. Bao, et al., Low-dose diet supplement of a natural flavonoid, luteolin, ameliorates diet-induced obesity and insulin resistance in mice, Mol. Nutr. Food Res. 58 (2014) 1258–1268.
[79] K. Fuenzalida, R. Quintanilla, P. Ramos, D. Piderit, R.A. Fuentealba, G. Martinez, et al., Peroxisome proliferator-activated receptor gamma up-regulates the Bcl-2 anti-apoptotic protein in neurons and induces mitochondrial stabilization and protection against oxidative stress and apoptosis, J. Biol. Chem. 282 (2007) 37006–37015.
[80] S. Nie, Z. Shi, M. Shi, H. Li, X. Qian, C. Peng, et al., PPARγ/SOD2 protects against mitochondrial ROS-dependent apoptosis via inhibiting ATG4D-mediated mitophagy to promote pancreatic cancer proliferation, Front. Cell Dev. Biol. 9 (2021), 745554.